

Catskill Mountain Water Resources: Vulnerability, Hydroclimatology, and Climate-Change Sensitivity

Allan Frei,* Richard L. Armstrong,** Martyn P. Clark,** and Mark C. Serreze**

**Department of Geography, Hunter College, The City University of New York*

***Cooperative Institute for Research in Environmental Sciences, National Snow and Ice Data Center, University of Colorado*

We present an initial assessment of the potential impact of climate change on water supply in the Metropolitan East Coast (MEC) region of the U.S. National Assessment of the Potential Consequences of Climate Variability and Change. A version of the Thornthwaite water-balance model is applied to one of six basins in the Catskill Mountains that together provide water for approximately 10 million people in New York City and other municipalities. In addition to Thornthwaite's original soil moisture reservoir, the model includes the snow pack water reservoir of Willmott, Rowe, and Mintz (1985), a ground-water storage term, and several additional modifications. Following a review of the vulnerability of water supplies and historical hydroclimatology of this region, we estimate (1) the sensitivity of water supply to altered temperature and precipitation regimes and (2) the potential impacts of specific climate-change scenarios used by national and regional climate-change assessments. The sensitivity of runoff to temperature changes is approximately 6 percent per degree C; its sensitivity to precipitation changes is approximately 1.5–2 percent per percent change in precipitation, for annual mean values. Under all scenarios, rising temperatures will lead to significantly diminished water supplies unless precipitation increases dramatically. Due to disagreement between precipitation projections from different models and scenarios, projected changes in mean annual water supply range from approximately +10 percent to –30 percent by the 2080s. Under the driest scenario, water supplies under mean climatic conditions will be comparable to the worst extended drought period of the twentieth century in this region. Equally important are the likely effects on the annual cycle, which include an earlier peak runoff and a reduction of the snowpack by at least 50 percent. Considered in the context of likely increased demands, these changes may be significant. *Key Words:* hydroclimatology, New York, water balance, water supply.

The U.S. National Assessment of the Potential Consequences of Climate Variability and Change, organized under the auspices of the U.S. Global Change Research Program, contains eighteen regional components. The Metropolitan East Coast (MEC) regional assessment, the smallest and most densely populated region, covers thirty-one counties in the New York City metropolitan area. A stated objective is to identify “sectors that are vulnerable to the additional stresses that increased climate variability will introduce and the potential for adaptation strategies to cope with them” (Rosenzweig and Solecki 2001b; see also Rosenzweig and Solecki 2001a).

The MEC assessment is organized around seven sector studies, one of which is water supply. Much of the assessment relies on results from general circulation model (GCM) experiments developed for use by the Intergovernmental Panel for Climate Change (IPCC). In addition to identifying temperature- and precipitation-change scenarios for the coming century, the assessment makes conclusions about each sector, including six key

conclusions regarding water supply, summarized here (Rosenzweig and Solecki 2001a):

- The natural variability of the hydrologic systems in the region will increase, with potential increases in both floods and droughts.
- Increased uncertainty will require a range of resiliency options from water management.
- Ecosystem services are likely to be affected.
- New York City's water-supply systems should be able to cope with climate uncertainty over the very near term, but an effective planning process needs to be put in place in order to consider the adaptations that may be required in the future.
- The implementation of institutional and infrastructure measures is likely to require long-term institutional commitments.
- Interregional cooperation may offer opportunities to utilize water resources more efficiently.

Up to this stage of the assessment, however, no effort has been made to quantify the potential impacts on

water supply. The analysis laid out in this article is a first step in that direction. We present a variation of the Thornthwaite method for estimating soil moisture and water balance. This method is designed for basins with significant relief and seasonal snow pack. It requires only standard meteorological observations—including daily temperature, precipitation, and snowfall—and is therefore applicable in many basins across the U.S. and the globe. We use temperature and precipitation projections from GCMs adopted by the national and regional assessments to examine specific scenarios of climate change. Similar methods have been applied in nearby regions and elsewhere (Wolock et al. 1993; Arnell 1996; Wolock and McCabe 1999a).

The Catskill Mountains are a region of social and economic significance, supplying water to approximately 10 million people in New York City as well as in other New York and New Jersey municipalities. Control of Catskill watersheds is also critical to Philadelphia, due to the effect of these watersheds on salinity in the lower Delaware River. Yet, to our knowledge, there exists a dearth of reporting on the Catskills in the geographic literature. Therefore, we provide some background regarding the vulnerability of the water supply and the historical hydroclimatology of these watersheds, in addition to examining their sensitivity to climate change.

The Catskills are actually the eastern end of the Allegheny Plateau. Peaks over 1000 m are found in three primary ridge systems that run roughly west/northwest to east/southeast. As shown in Figure 1, the New York City water supply system relies primarily on six Catskill basins: the Ashokan, Schoharie, Rondout, Neversink, Cannonsville, and Pepacton. Each has an associated reservoir (in this section of the article, the term "reservoir" refers to the actual water body that collects water, not to the water storage terms referred to as "reservoirs" in the model description), which together provide 90 percent of the city's water. The eastern or "Catskill" system, including the Ashokan and Schoharie basins, drains naturally into the Hudson River and supplies 40 percent of the city's water. The Ashokan reservoir has been supplying water since 1915. The western or "Delaware" system, including the remaining basins, constitute the headwaters of the Delaware River, although these waters are diverted into the reservoir that impounds Rondout Creek, which drains naturally into the Hudson. The Delaware system, which currently supplies 50 percent of the city's water, came on line in 1965 in the midst of the driest extended period (in terms of streamflow levels and precipitation rates) of the century. The "Croton system" (not shown) includes reservoirs in and around Westchester County just north of New York City. It is the oldest part of the

system, supplying the remaining 10 percent of the city's water. This system lies outside the domain of this study.

The climate of the Catskills is characterized by a pronounced seasonal cycle of temperature, but not of precipitation. Typically, total precipitation is 1000–1200 mm yr⁻¹, with snowfall accounting for approximately 20 percent of total water equivalent. A southeast-to-northwest gradient in temperature and precipitation reflects the moderating influence of the Atlantic Ocean and the varying effects of coastal and continental storm systems superimposed on the latitudinal gradient. In addition, orography influences the spatial distributions of precipitation and temperature. Thaler (1989, 1994, 1996) has described the climate of this area (his 1996 volume is of particular interest). Our focus is on the Cannonsville watershed in the Delaware system. To point out differences between the eastern and western portions of the study area, we also present selected results from the Ashokan watershed.

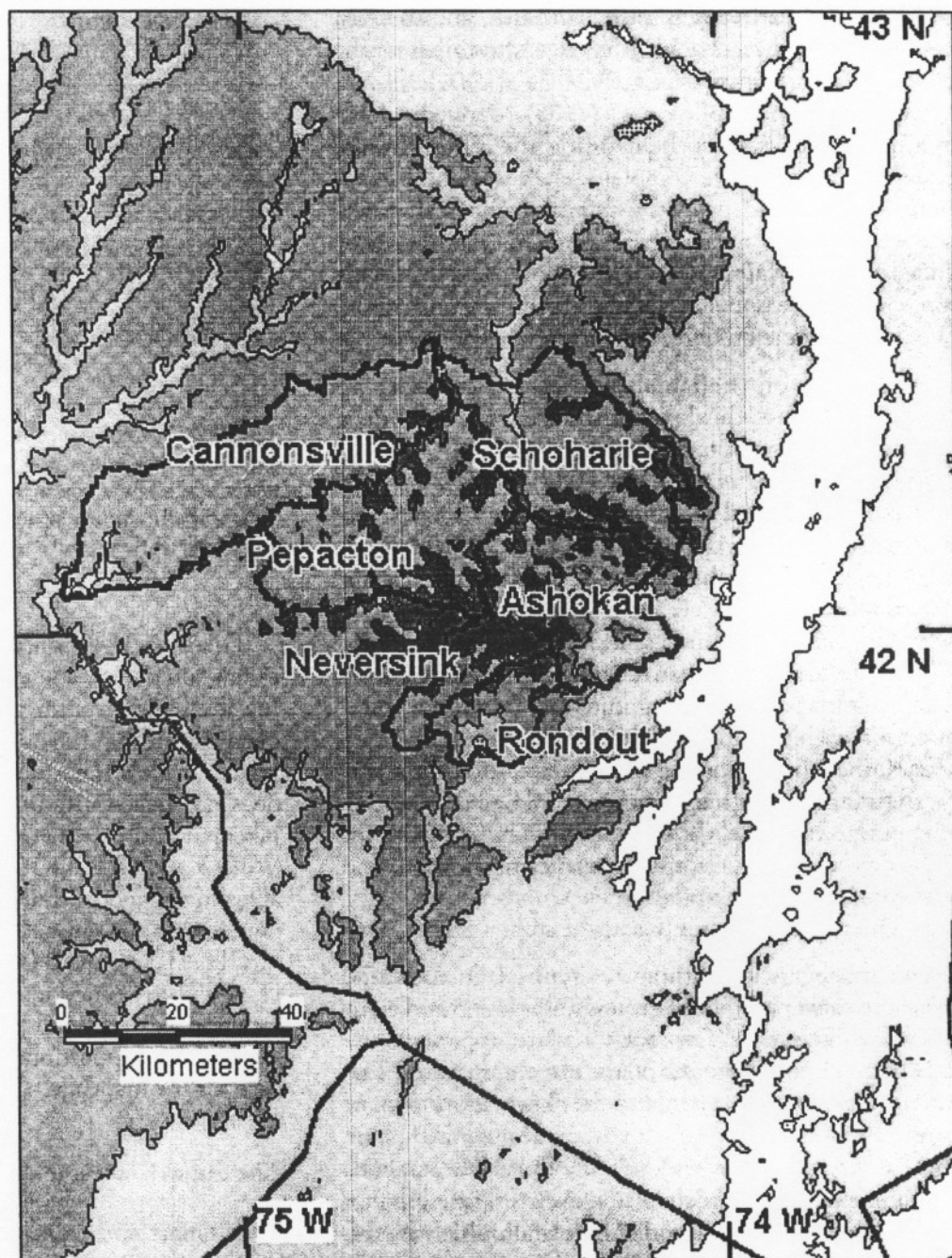
In the next section of this article, we discuss model formulation, initialization, and validation. In the third section, we describe the data and GCM output used as input to the water-budget model. In the fourth and fifth sections, we discuss the vulnerability of water supplies to environmental stresses in this region and the region's historical hydroclimatology. The sixth section is devoted to the anomalous hydroclimatology of two periods of particular interest, the dry 1960s and the wet 1970s. In the seventh section, the sensitivity of Catskill water supplies to climate change is discussed, followed by summary and conclusions in the final section. Readers not interested in modeling and data details can skip the second and third sections.

Water-Budget Model: Formulation, Initialization, and Validation

Model Formulation

In the 1940s, Thornthwaite (1948) developed a simple but elegant empirical method for estimating daily soil moisture, evapotranspiration, and surplus with the intent of estimating global fields of the water balance. The sole water reservoir in his original model is the root zone, the uppermost soil layer accessible to vegetation from which evapotranspiration occurs. Subsequently, Thornthwaite and Mather (1955, 1957) used this method to provide monthly evapotranspiration, soil moisture, and surplus estimates over many regions of the globe using station observations of temperature and precipitation. The basic model has since been used and modified numerous times (e.g., Muller 1969, 1981; Mather 1981, 1985, 1992; Willmott, Rowe, and Mintz 1985; McCabe

Figure 1. Topographic map of the Catskill region and the six watersheds that supply 90 percent of New York City's water. Region covers between 73.5W and 75.5W longitude and 41N and 43N latitude. The Schoharie and Ashokan comprise the "Catskill System," while the Cannonsville, Pepacton, Neversink, and Rondout comprise the "Delaware System." Elevations are: <100 m (white); 100 m to 400 m (light shade); 400 m to 700 m (medium shade); 700 m to 1000 m (dark shade); and >1000 m (black). The area with elevation <100 m is mostly the Hudson River valley.



and Ayers 1989; Legates and Mather 1992; Mintz and Serafini 1992; Wolock et al. 1993).

Although more than fifty years old, Thornthwaite's empirically derived relationships remain a valuable tool. To calculate evapotranspiration directly requires estimating the surface energy budget, for which measurements of surface radiative and turbulent heat fluxes are necessary. During Thornthwaite's time and to this day, such measurements are generally scarce. Several recent studies have compared a number of potential evapotrans-

piration routines and found Thornthwaite to work as well as others for broadleaf forests (Vorosmarty, Federer, and Schloss 1998) and midlatitude locations (Federer, Vorosmarty, and Fekete 1996) and in comparison to methods utilizing surface radiation fluxes (Mintz and Walker 1993). None of the aforementioned studies included the potentially important effects of changing carbon dioxide concentrations on plant physiology (Martin, Dickinson, and Yan 1999). However, Lockwood (1999) contends that this effect is likely to be small in

moist, forested areas such as the Catskills, and that uncertainties in the feedbacks are currently too great for the effect to be quantified accurately.

Willmott and colleagues (1985) derived global monthly water balance fields using the Thornthwaite equations with a more complete set of station observations and updated evapotranspiration and soil water-storage capacity parameterizations. In addition they added a second water reservoir, the snow pack, to provide more realistic seasonal cycles of soil moisture and runoff. We use their version here, but with several changes:

- Building on their inclusion of a snow pack, we introduce a third water-storage reservoir: deep groundwater storage. Associated with the groundwater storage term are two additional water fluxes: percolation and base flow. Inclusion of a deep storage term allows the estimation of base flow and has some effect on the timing of the seasonal stream-flow cycle.
- The model is run in a semidistributed mode appropriate for use in basin-scale studies by accounting for variations of temperature and frozen precipitation with elevation.
- Rather than assuming that precipitation for a particular day is either all frozen or all liquid, we incorporate observations of snowfall. This provides for improved distinctions between rain, snowfall, and mixed phase precipitation.
- The model is run for daily time steps.

Our model includes three reservoirs (the root-zone layer, the snow pack, and a groundwater layer) and eight flux terms (Figure 2). The root-zone layer represents the soil up to a depth where the plants can obtain water. The groundwater reservoir simulates the slower movement of water through deeper soil layers associated with base flow, as opposed to over-land runoff, which responds more immediately to precipitation events. The eight flux terms include (1) rainfall and (2) snowfall, which are the model inputs obtained from observations. Snow melt (3) is added to rainfall to calculate the total input into the root-zone layer. Fluxes out of the root-zone layer include (4) evapotranspiration, (5) percolation into the deep layer, and (6) surplus, which represents over-land runoff. Groundwater storage is determined by the balance between percolation and groundwater runoff, or (7) base flow. Base flow is added to surplus to estimate (8) total runoff, which can be compared to observed stream-flow. Note that infiltration into the root zone and uptake by the plant roots are assumed to be unrestricted, and no terms are included for interflow or bank storage. Table 1 provides a list of model variables.

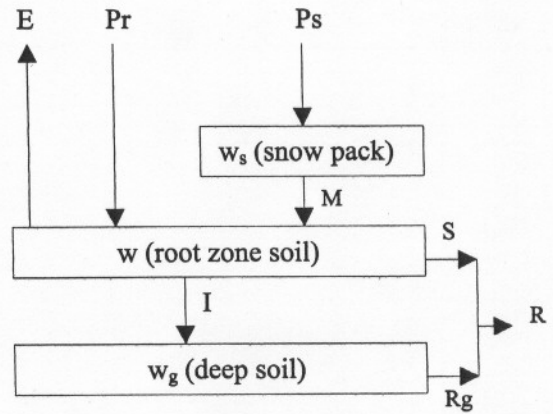


Figure 2. Water balance model reservoirs and flux terms. Reservoirs include w_s (snow pack), w (root-zone layer), and w_g (groundwater layer). Flux terms include ET (evapotranspiration), P_r (rain), P_s (snowfall), M (snow melt), S (surplus), I (percolation), R_g (groundwater flow), and R (total runoff).

This model was constructed with the goal of including as few tunable parameters as possible, while still capturing the basic physical processes described above. It has been shown that the addition of complexity into hydrological models (i.e., inclusion of additional parameters) does not necessarily improve results (Andersson 1992; Jakeman and Hornberger 1993; Lindstrom et al. 1997; Wolock and McCabe 1999b). Therefore, of the five variables in the model that could potentially be used as parameters, in the sense that their values could be tuned— a_{melt} , H_g , H_l , w^* , and β (see Table 1 for definitions)—only H_g and H_l are tuned in this analysis. Appropriate values for w^* , a_{melt} , and β are taken from other sources. Below, we describe the portions of our model that are presented here for the first time.

The Snow Reservoir

Willmott and colleagues (1985) calculated snowfall by assuming that if the daily mean temperature is below freezing, then all precipitation for that day is frozen; otherwise, it is liquid. It would have been impractical for them to incorporate observed snowfall into global scale calculations due to the dearth of observations. However, since daily snowfall data are available for many sites across the U.S., we devised a method to include these observations in partitioning total precipitation into its frozen and liquid components.

Since snowfall is recorded in units of depth, in the absence of concurrent snow-density measurements, snowfall and total precipitation measurements are incompatible. To incorporate snowfall data, we developed a

Table 1. Variables Used in the Water-Balance Model

Variable	Definition	Units
a_{melt}	Melt parameter	mm °C ⁻¹ day ⁻¹
A	Empirical exponent used in calculation of PE	none
c_r	Exponential decay constant for deep water runoff	day ⁻¹
c_l	Exponential decay constant for percolation	day ⁻¹
ET	Daily evapotranspiration	mm day ⁻¹
H	Daily number of hours of daylight	hours
H_g	Half-life for exponential decay for deep water runoff	days
H_l	Half-life for exponential decay for percolation	days
I	Daily percolation, or flow from root zone to deep groundwater	mm day ⁻¹
i	Monthly temperature index associated with T_m , used to calculate I_T	none
I_T	Annual temperature index associated with monthly values of I	none
M	Snow melt rate	mm day ⁻¹
P	Total daily precipitation = $P_r + P_s$	mm day ⁻¹
PE	Daily potential evapotranspiration	mm day ⁻¹
P_r	Daily rainfall	mm day ⁻¹
P_s	Daily snowfall	mm day ⁻¹
R	Total daily runoff = $R_g + S$	mm day ⁻¹
R_g	Daily deep water runoff, or base flow	mm day ⁻¹
S	Daily surplus, or overland flow	mm day ⁻¹
t	Time	days
T	Daily mean temperature	°C
T_m	Monthly mean temperature	°C
w	Root-zone soil water-storage reservoir	mm water equivalent
w^*	Root-zone soil water-storage capacity	mm water equivalent
w_g	Deep-ground water-storage reservoir	mm water equivalent
w_s	Snow pack water-storage reservoir	mm water equivalent
β	Parameter that defines the dependence of ET on w and w^*	none

decision tree. Using observations of snowfall, total precipitation, and temperature, we estimated the density and snow water equivalent (SWE) of new snow in a way that is consistent with physical principles and observed densities and ensures that the observations from each station are internally consistent. The density of new snow is

estimated by dividing total precipitation (mm depth) by measured snowfall (mm depth) and multiplying by water density (1000 kg m⁻³). The rules are as follows:

1. If the estimated density of new snow is between 50 and 250 kg m⁻³, we assume that all precipitation fell as snow. In this case, SWE is equal to precipitation and rainfall is set to zero.
2. If no precipitation is recorded, but snowfall is greater than 0, a snow density of 100 kg m⁻³ is assumed. Precipitation is set equal to SWE, and rainfall is set to zero. This partially addresses the problem of snowfall undercatch.
3. If the density of new snow is less than 50 kg m⁻³, we again assume snowfall undercatch. We set density equal to 50 kg m⁻³, set precipitation equal to SWE, and assume no rainfall.
4. If the density of new snow is greater than 250 kg m⁻³, it is assumed that precipitation fell as a mixture of rain and snow. The density of new snow is set to 250 kg m⁻³, and the remainder of the precipitation is taken to fall as rain.
5. If the daily maximum temperature is below freezing, and as a result of steps 1 through 4 estimated SWE is less than total precipitation (i.e., rainfall > 0), snowfall is set equal to total precipitation and rainfall is set to zero. Conversely, if the daily minimum temperature is above freezing, and snowfall is greater than 0, we set rainfall equal to total precipitation and set snowfall to zero.

Results from this procedure were compared to the raw precipitation totals from six first-order stations near the Catskills (see section below on "Data and GCM Output"). At most stations, this resulted in maximum monthly changes of $\cong 4$ percent and mean snow densities of approximately 110 kg m⁻³. For a discussion of snow densities observed at high-elevation sites in the Rocky Mountains, from which the values used in this decision tree were obtained, see Judson and Doesken (2000) and Doesken and Judson (1997).

Groisman and Legates (1994) and Legates and DeLiberty (1993) estimate the magnitude of the precipitation undercatch problem across the eastern U.S. (including the Catskills), with summer mean biases of 5–7 percent, winter undercatch possibly three times higher, and annual mean biases in the region estimated to be 10–14 percent. Legates and Mather (1992) recommend that when using the Thornthwaite evapotranspiration routine, uncorrected precipitation data be used, as the Thornthwaite equations were derived using uncorrected values. Hence, only the minor corrections described above, which mostly ensure that precipitation and snow-

fall observations are internally consistent, are utilized. For snow melt, we use the parameterization used by Willmott and colleagues (1985), which includes terms for precipitation and temperature. Using observed SWE at the Albany, New York first-order station, we compared this melt parameterization favorably against the simplest parameterization, the temperature index method, using a range of typical index values between 3 and 6 mm C⁻¹ day⁻¹ (Kustas, Rango, and Uijlenhoet 1994).

Soil Water Storage

An important parameter for which a value must be chosen is the root-zone water-holding capacity (w^*), the derivation of which is discussed by Mintz and Walker (1993) who use a value of $w^* = 150$ mm, consistent with estimates by McCabe and Ayers (1989) for the Delaware River Basin and Karl (1983) for the eastern United States. While typical values are in the range of 100–280 mm depending on soil and vegetation conditions, Milly (1994) finds that values greater than 150 mm have only minor effects on results. We use 150 mm in this study.

Groundwater Storage

The only difference between our root-zone formulation and that of Willmott and colleagues (1985) is that we include a term for percolation into the deep storage reservoir. This term improves estimates of the seasonal cycle of streamflow. In our model, w_g is calculated as a balance between percolation from the root-zone layer (I) and runoff from the deep layer (R_g):

$$\frac{\partial w_g}{\partial t} = I - R_g \quad (1)$$

Both I and R_g are modeled as exponential decay functions:

$$I = c_1 w_{i-1} \quad (2)$$

$$c_1 = \frac{0.693}{H_1} \quad (3)$$

where c_1 (day⁻¹) is the percolation constant, w_{i-1} is the root-zone moisture of the previous day, and H_1 is the percolation half-life, which represents the number of days after which the root-zone layer would be 50 percent depleted by percolation in the absence of rain, snow melt, or E. If calculated percolation is greater than the water available in the root zone, then I is set to the maximum soil water available. R_g is estimated as an exponential decay function, similar to I . The half-lives of the two soil layers are fitted to observed flow during summer when the contribution of precipitation is minimal.

Alley (1984) reviews several methods to incorporate w_g into monthly water balance models. Alley's "abcd" method includes a groundwater runoff term with similar characteristics to the one chosen here, although Alley's terminology is different. Our values are consistent with those identified in Alley's abcd model.

Total runoff is simply the sum of base flow (R_g) and over-land flow (S):

$$R = R_g + S \quad (4)$$

Figure 3 shows the effect of the groundwater storage term (using half lives of $H_1 = 180$ days and $H_g = 120$ days) on estimated streamflow. Both models capture the basic shape of the observed seasonal cycle with a spring peak and a secondary early winter peak. The primary deficiency in the model is the early peak in the spring runoff. The addition of w_g has two primary effects. First, base flow increases summer streamflow from almost zero to more realistic magnitudes. Second, the winter maximum is decreased and delayed. Most importantly, the groundwater term enables us to estimate base flow, and is therefore included in the model.

Initialization

With the exception of the groundwater terms described above, the water balance model requires no calibration (Thornthwaite's parameterizations were calibrated on observations from many locations in different

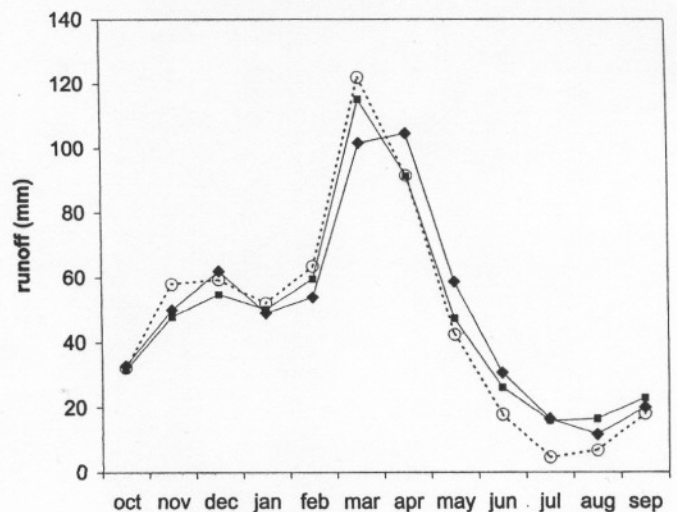


Figure 3. Monthly mean streamflow in the Cannonsville basin (1959–1988). Observations are shown with the solid line and solid diamonds. Model results, including a groundwater reservoir, are shown with the solid line and solid squares. Model results with no groundwater reservoir are shown with the dashed line and open circles.

climates). The model is initialized by setting w , w_s , and w_g to 100 mm, 0 mm, and 70 mm, respectively. These values were specified from mean model results of preliminary runs, and the spin-up period of one year is sufficient so that results are not sensitive to reasonable changes in initial values. The model in the present configuration can be run only for days when observed precipitation, snowfall, and maximum and minimum temperatures are available.

We use a temperature adjustment for elevation assuming a nominal 7°C km^{-1} environmental lapse rate. Leffler (1981) calculated lapse rates using two stations in New Hampshire and found seasonal values lower than this. Sensitivity tests indicate that the model is relatively insensitive to values between 6°C km^{-1} and 7°C km^{-1} .

Elevations in the Cannonsville basin taken from the digital elevation model (DEM) range between 350 m and 950 m (Figure 4). The meteorological station lies in the lowest elevation category. The distributed model is run once at each of the twelve elevation bands at +50-m increments, which correspond to -0.35°C increments. Results from all twelve runs are weighted according to the number of pixels in each elevation band and averaged to derive basin-mean values.

The elevation correction does not affect total precipitation amount, but does affect the proportion falling as snow, the rate of snow melt, the timing of the peak melt, and the evaporation rate. However, it is likely that the amount of total precipitation does in fact increase with elevation (e.g., Hendrick and DeAngelis 1976). While inclusion of this effect would improve the seasonal timing of runoff, which in the model peaks slightly early in

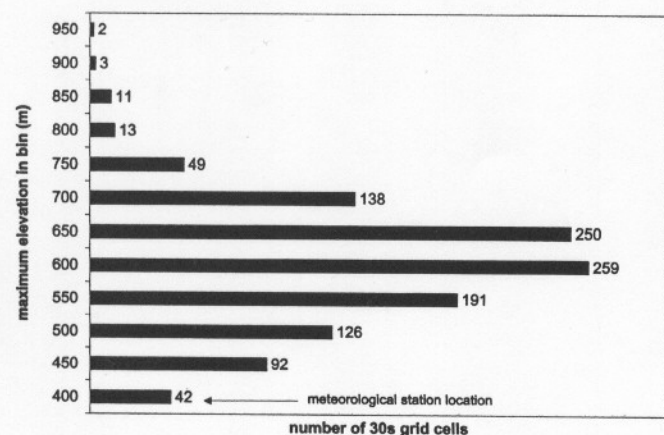


Figure 4. Elevation bar-chart for the Cannonsville watershed. Each value represents the number of grid cells in 50 m bins (e.g., there are 259 grid cells with elevation $550 < h \leq 600$ m). There are a total of 1176 grid cells in the basin. The elevation of meteorological station #308963 is indicated.

spring (see Results section below), this is excluded to minimize model tuning. A more detailed analysis of Catskills lapse rates is reserved as a potential method for future model improvement.

Validation

Figure 5 shows scatter plots of observed versus modeled annual and monthly streamflow for the Cannonsville basin. The model tends to underestimate mean and high runoff years and overestimate low runoff years (Figure 5A). Nevertheless, the correlation of 0.97 between modeled and observed annual runoff indicates that the model does an excellent job of capturing interannual variability. In this basin, the correlation between precipitation and observed streamflow is 0.91. Thus, the model explains significantly more variance than if we used observed precipitation as a proxy for runoff. Mather (1981) compared his results to measured streamflow over basins on the Delmarva peninsula on the mid-Atlantic coast of the eastern U.S. For basins over which he rated the

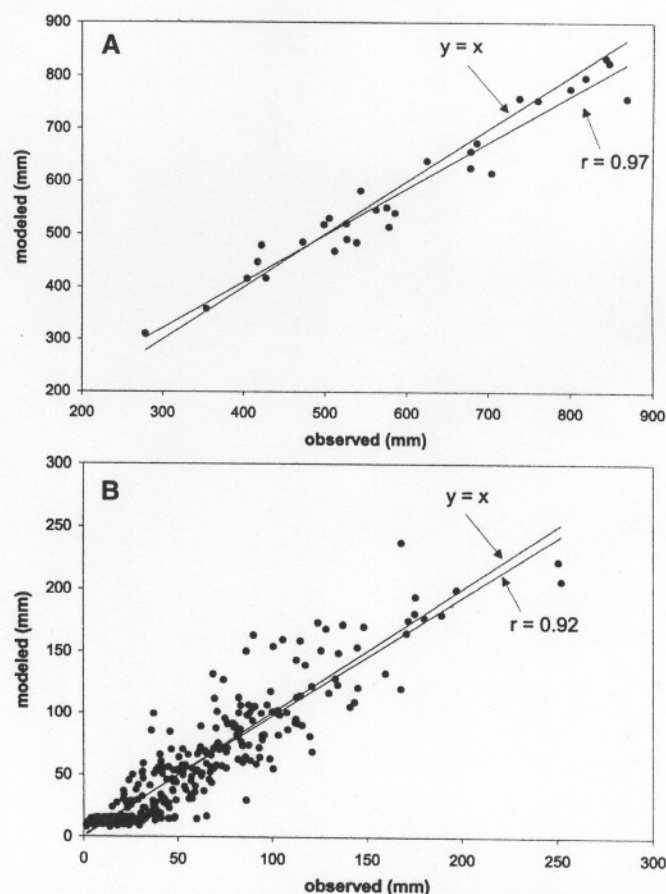


Figure 5. Observed versus modeled streamflow for (A) annual and (B) monthly values.

model results in his best category, he found correlations ranging from 0.81 to 0.93 for *monthly* streamflow over a three-year simulation. Figure 5B shows the monthly scatter plot for the Cannonsville basin, for which the correlation is 0.92 over a thirty-one-year simulation. However, in both this case and Mather's, such high correlations are misleading, because the seasonal cycle has not been removed. To remove this effect, we correlated runoff for each month individually. Over the Cannonsville basin for individual months the correlations range from 0.77 to 0.96, with only summer (June, July, and August) correlations falling below 0.86.

Data and GCM Output

In this section, we describe the meteorological observations, digital elevation data, and output from GCMs used in this analysis. The water-budget model requires daily inputs of temperature, precipitation, and snowfall. Annually averaged results are reported for the U.S. Geological Survey (USGS) water year (October through September) and are referred to by the year in which they end (e.g., water year 1996 ends in September 1996). Table 2 provides information on the stations.

NWS Cooperative Station Observations

Data from cooperative weather stations are managed by the National Weather Service (NWS). Trained volunteers using standard NWS instruments measure precipitation, snowfall, snow depth, and maximum and minimum temperatures. Data are sent to the National Climatic Data Center in Asheville, North Carolina, where they are digitized, quality-controlled, and archived. We primarily use observations from one station for each watershed. The station at Walton, New York (station #308936) is used to calculate the water budget for the Cannonsville watershed. The station at Slide

Mountain, New York (station #307799), is used to calculate the water budget for the Ashokan watershed.

NWS First-Order Station Observations

NWS employees take meteorological data from first-order stations, which are often located at airports. These data include observations in addition to those taken at cooperative stations. Data from the first order station at the airport in Albany, New York (zero missing months) is used for development of the snow-melt routine. We use daily maximum and minimum temperature, precipitation, snowfall, snow depth, and SWE for January 1946 through December 1997. The records were obtained from the Northeast Regional Climate Center in Ithaca, New York.

USGS Stream Gauge Observations

Stream flow data from USGS gauge stations were taken from the Hydroclimatic Data Network (Slack, Lumb, and Landwehr 1993). The archive includes stations with no diversions or other flow alterations, which are therefore useful indicators of climatic and land-cover changes. The primary station used in this analysis is located near the base of the Cannonsville watershed on the West Branch of the Delaware River at Walton, New York (zero missing months). We convert discharge data (cubic feet per second) to runoff (mm) in order to facilitate comparisons to precipitation and between basins of different sizes.

Digital Elevation Data

Digital elevation data were obtained from the USGS GTOPO30 Global 30 Arc Second Elevation Data Set, which is a global DEM with a horizontal grid-spacing of 30 arc-seconds (approximately 1 kilometer). These data are available on the World-Wide Web from the USGS

Table 2. Stations Used in This Analysis^a

Type of Station	Station Number	Station Name	Latitude (N)	Longitude (W)	Elevation (m)	Period of Record
NWS cooperative	307799	Slide Mountain	42.02	74.42	807	1963–1997 (fourteen missing months)
NWS cooperative	308936	Walton	42.17	75.13	378	1957–1997 (one missing month)
NWS first-order	n.a.	Albany County Airport	42.75	73.80	84	1946–1997
USGS stream-gauge	01423000	West Branch Delaware at Walton	42.17	75.14	n.a.	1950–1988

Note: n.a. indicates not available.

^aThis includes two cooperative weather stations, one National Weather Service first-order station, and one USGS stream gauge station.

Earth Resources Observation Systems Data Center Distributed Active Archive Center (2001).

GCM Output

The MEC assessment uses five potential scenarios in its analyses. For the first scenario, it is assumed that linear trends calculated from observed regional temperature and precipitation records during the twentieth century will continue into the twenty-first century (current trend). The other four scenarios (HHGG, HHGS, CCGS, and CCGG, described below) are taken from the results of climate model experiments.

The national and regional assessments adopted modeling results from two of the IPCC modeling groups, the U.K. Hadley Centre for Climate Prediction and Research and the Canadian Centre for Climate Modelling and Analysis. Information on these model experiments was obtained on the IPCC's Web site, on which more detailed information, as well as model output and additional references, are available. For our analysis, we obtained temperature and precipitation values from the model grid cell located most nearly above the basin. Thus, the temperature and precipitation scenarios used here differ slightly from those quoted in the MEC report because the Cannonsville Basin is located slightly to the northwest of the MEC region. Note that all model scenarios except CCGG are the mean results of ensemble experiments.

The Hadley Centre model (Hadcm2, referred to as HH in this report) is a coupled atmosphere-ocean GCM with a common spatial resolution 2.5×3.75 (latitude, longitude) in both the atmosphere and ocean components and an equilibrium climate sensitivity of approximately 2.5°C , although this quantity varies with the time-scale considered. This is somewhat lower than most other GCMs. HH experiments were performed with forcing beginning in the middle industrial era, about 1860. The greenhouse-gas-only integrations (HHGG) used the combined forcing of all the greenhouse gases as an equivalent CO_2 concentration. A further series of integrations (HHGS) used the combined equivalent CO_2 concentration plus the negative forcing from sulphate aerosols. The direct radiative forcing due to anthropogenic sulphate aerosols is represented in the model by means of an increased clear-sky surface albedo proportional to the local sulphate loading.

The Canadian Climate Center model (CC) is a spectral model with triangular truncation at wave number 32, yielding a surface-grid resolution of roughly $3.7^\circ \times 3.7^\circ$. This is coupled with an ocean component with resolution $1.8^\circ \times 1.8^\circ$. An ensemble of four transient climate-

change simulations has been performed. Three of these simulations (CCGS) use an effective greenhouse-gas-forcing change corresponding to that observed from 1850 to the present, and a forcing change corresponding to an increase of CO_2 at a rate of 1 percent per year (compounded) thereafter until year 2100. The direct forcing of sulphate aerosols is also included by increasing the surface albedo by an amount based on results of a previously published sulphur cycle model. The fourth simulation considers the effect of greenhouse-gas forcing only (CCGG). The climate sensitivity of the CC model is about 3.5°C .

Water-System Vulnerability

The New York City water-supply system involves an extensive network of reservoirs and tunnels that transfer water over 160 km (100 miles) from upstate watersheds to downstream consumers, including approximately 8 million New York City residents and more than 1 million upstate residents. The Delaware watershed is also critical to users in New Jersey and Pennsylvania. This system has been built over the last 160 years, and though it has historically been a reliable source of high-quality water, it is vulnerable to a variety of stresses associated with water quality, supply and demand, and climate variability. Potential water-quality stresses include those associated with increased development in the watersheds, both point and nonpoint sources of pollution (NRC 2000), and with acid rain (Burns, Lawrence, and Murdoch 1998). The system relies on natural filtration processes in the watersheds to maintain water quality. No New York City water is currently processed through filtration plants, although the city has agreed to filter Croton water. In the 1990s, a highly publicized and heated series of political battles and negotiations between upstate residents and New York City officials occurred as a result of a 1989 federal Environmental Protection Agency (EPA) ruling. The reservoirs were deemed to be vulnerable to water-quality problems, and under the EPA's Surface Water Treatment Rule the city was ordered to either develop a plan to ensure long-term ecological protection of the watersheds or build a filtration plant. A filtration plant with sufficient capacity to process Catskill and Delaware water would require an initial outlay of several billion dollars, plus several hundred million dollars per year in operation and maintenance costs.

Stresses related to supply and demand are of further concern. With a total watershed area of close to 5000 km^2 (2000 square miles) and a total capacity of approximately $2 \times 10^9 \text{ m}^3$ (500 billion gallons) this network cur-

rently supplies 5×10^6 m³/day (1.3 billion gallons per day [bgpd]), and up to 7.5×10^6 m³/day (2 bgpd) at peak usage. Thus, the storage capacity of the system is equal to only about a one-year supply.

During the latter half of the twentieth century, the system experienced significant fluctuations in climate, water supply, and demand. Figure 6 shows streamflow from two gauge stations in the Catskills with long, unbroken records. The two periods of most extreme, persistent streamflow anomalies of the century were the early to mid-1960s deficit and the abundant years of the mid-1970s. Corresponding precipitation time series are shown in Figure 7. In June 1961, the city's reservoirs were full, but by November 1963 storage had dropped to 26 percent of capacity (Groopman 1967). During the following five or so years, except for a brief period in 1964, drought conditions were severe. During that time, consumption was reduced through a combination of mandatory restrictions and voluntary measures and through an intensive public education campaign (Groopman 1967).

From the mid-1960s to around 1980, the system experienced a marked increase in demand from under 4.2×10^6 m³/day (1.1 bgpd) to approximately 5.7×10^6 m³/day (1.5 bgpd) that coincided with increased availability. Several periods during which New York City and downstream users of Delaware water experienced drought problems in the early 1980s occurred when the water-supply deficit was not nearly as severe as fifteen years prior. Yet reservoir levels dropped precipitously because of the dramatic increase in consumption (Weisman 1985): the population had come to rely on the abundant

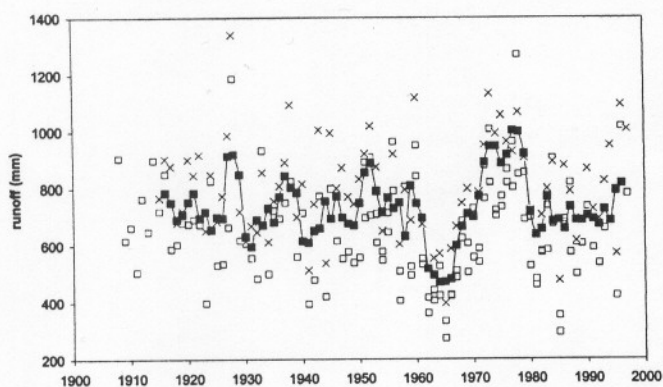


Figure 6. Annual runoff (streamflow normalized by basin drainage area) in the Catskills. USGS gauge station #1423000, used in this analysis, is shown with open squares. Longer-term records are shown from Schoharie Creek at Prattsville, USGS #1350000 (open squares) and the East Branch of the Delaware River at Margaretville, USGS #1413500 (×). Also shown is the three-year running mean of the average of the two long-term stations (closed squares with line).

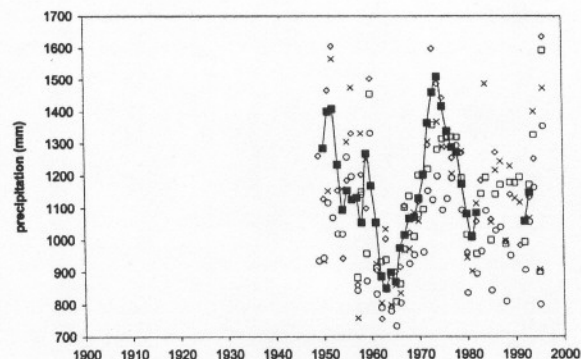


Figure 7. Annual precipitation in the Catskills. Cooperative station #308936, used in this analysis, is shown with open squares. In addition, records are shown from Grahamsville #303365 (open diamonds), Ellenville #302582 (×), and Stamford #308160 (open circles). Three additional stations are shown: of seventeen regional stations that include at least twenty-five years of data between 1964 and 1993, these three correlate highest to the other fourteen. Also shown is the three-year running mean for station #303365 (closed squares with line).

supplies of the 1970s. Since 1980, the nationwide trend has been towards declining withdrawals, with most savings having come in the power, industrial, and agricultural sectors (Gleick 2001). New York City withdrawals have also declined as result of a number of conservation measures that decreased consumption by about 15 percent (Goldstein and Izeman 1990), with average consumption during the early 2000s dropping to approximately 4.56×10^6 m³/day (1.2 bgpd). Nevertheless, since 1980 the city's water supply system has suffered a number of droughts (1980–1982, 1985, 1989, 1991, 1995, and 2001–2002) During the spring and summer of 1999, many parts of the mid-Atlantic suffered one of the driest seasons of the century. Although Catskills precipitation was below normal, the deficit was not as severe as it was farther south (Muller and McCabe 2000). While the summer of 2000 brought cool temperatures and abundant precipitation, the latter half of 2001 brought warm, dry weather to much of the eastern U.S. as a result of the frequent passage of high-pressure systems. In December 2001, the New York City Department of Environmental Protection (DEP) declared an official “drought watch” for the city's water supply system, and the Delaware River Basin Commission declared a “drought emergency,” which reduces New York City's allowable water withdrawals from the Delaware System (New York City DEP 2001). In late January 2002, the DEP upgraded the drought watch to a drought warning. At the time of this writing (February 2002), reservoir levels are less than 45 percent of capacity, far below the normal level (80 percent) for this time of year.

The results discussed in this report indicate that the system is also vulnerable to variations in water supply that may result during the twenty-first century as a result of climate fluctuations that are projected to be outside the range experienced during the twentieth century. In addition, rising sea level may affect neighboring ground water supplies (e.g., on Long Island), requiring additional consumption via interbasin transfers. In this analysis, we do not address water demand, water quality, management, or adaptation.¹

Hydroclimatology and Water Balance, 1959–1988

We focus on the water budget of the Cannonsville watershed. Rain and snow values reported here are from corrected observations (see the second section of this ar-

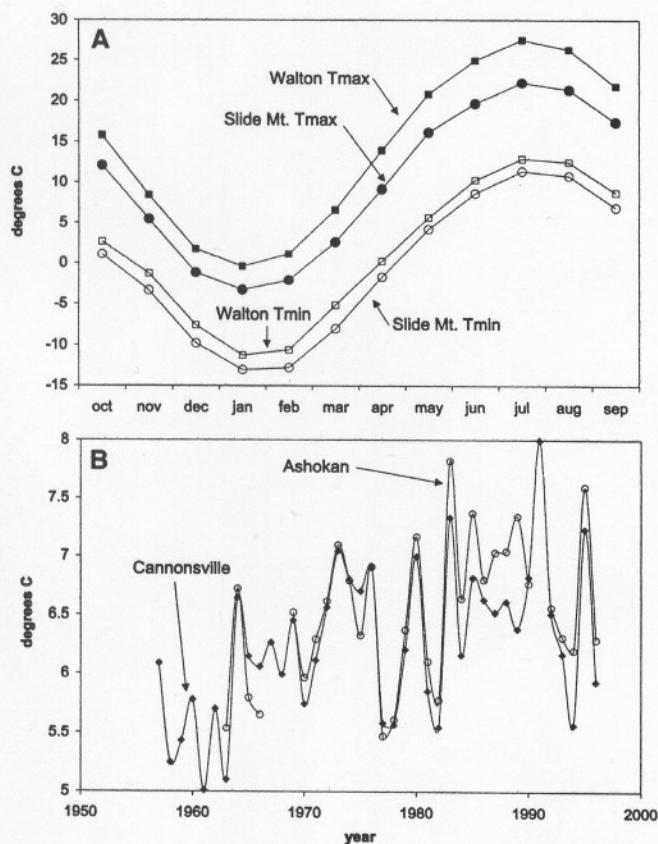


Figure 8. Mean temperatures in two Catskill basins. (A) Mean monthly (1964–1993) maximum and minimum temperatures at Walton (Cannonsville watershed, elevation 378 m) and Slide Mountain (Ashokan watershed, elevation 807 m). Values include no elevation corrections. (B) Annual mean temperatures over the Cannonsville (bold line) and Ashokan (solid line) watersheds based on elevation corrections.

ticle, above). All other flux values are calculated using the water-balance model. To illustrate differences between the western and eastern portions of the study area, we also show selected results for the Ashokan basin. For the latter basin, we use meteorological observations from Slide Mountain. Because the Slide Mountain station is located at a fairly high elevation, total precipitation may be overestimated for this basin. Also, the station is located at the southeastern edge of the basin, a region with locally high precipitation. Differences in monthly mean temperature minima and maxima between the two stations (Figure 8A) reflect the effects of elevation, latitude, distance from the ocean, and local topography. The largest differences occur during summer for maximum temperatures. The Cannonsville watershed is farther north and farther inland, while the Ashokan has higher elevations. When temperatures are interpolated over all elevation bands in the watersheds, these two effects tend to cancel each other out, such that basin-wide mean temperatures are comparable for years before 1980 (Figure 8B). However, since the early 1980s the Ashokan basin has been warmer, the reason for which is not clear.

Annual Mean Results

Table 3 summarizes annual mean fluxes. Precipitation over the Cannonsville watershed is 1137 mm yr^{-1} , with 80 percent coming from rain and 20 percent from snow. Approximately 550 mm yr^{-1} , or half of total precipitation, is lost to ET. Over the Ashokan watershed, ET loss is comparable in absolute amount (but not when expressed as a percentage of total precipitation). In the Cannonsville, approximately 28 percent of the total runoff is derived from base flow, with the remainder from surface flow. Over the Ashokan, 17 percent of total runoff comes from base flow.

Table 3. Annual Mean Water Fluxes in the Cannonsville (1957–1997) and Ashokan (1963–1997) Watersheds

	P	P _r	P _s	ET	PE	R	R _g	E _s	R _s
Cannonsville									
mm	1137	897	240	548	571	588	167	45	195
% of P	100	79	21	48	50	52	15	—	—
Ashokan									
mm	1593	1305	288	558	577	1020	177	38	250
% of P	100	82	18	35	36	64	11	—	—

Note: Values are expressed as mm of water equivalent and as percentage of total precipitation. — indicates not applicable. E_s and R_s are evaporation from snow and runoff from snow, respectively. See Table 1 for explanation of all other variables.

Seasonal Cycle

Figure 9 illustrates the mean seasonal cycle of water fluxes over the Cannonsville watershed. Rainfall is $\cong 100 \text{ mm mo}^{-1}$ during summer and drops to 30 mm mo^{-1} during January and February. Snowfall is $\cong 50 \text{ mm mo}^{-1}$ during winter, or approximately 60 percent of total winter precipitation of $\cong 80 \text{ mm mo}^{-1}$. ET exceeds 100 mm mo^{-1} during summer and is negligible during winter. ET is slightly less than PE from July through September, when soil moisture drops to less than around 60 percent of capacity, compared to almost 100 percent of capacity during winter and spring. (Recall from the third section of this article that water capacity is taken as 150 mm.) These results are consistent with global field estimates by Mintz and Serafini (1992), Mintz and Walker (1993), and Willmott and colleagues (1985). Groundwater storage is less variable than root-zone moisture, peaking in spring at $\cong 90 \text{ mm}$ and lowest in autumn at $\cong 70 \text{ mm}$. As a result of interactions between these fluxes, the annual streamflow cycle has a primary peak in spring and a secondary peak in winter. Differences between observed streamflow and calculated runoff are ≤ 20 percent.

Table 4 summarizes the interannual variability for each season. Standard deviations for seasonal temperature are typically between 0.9 and 1.3°C but are higher for winter minimum temperature (1.9°C). For annual temperatures, the standard deviation is less than 1°C . For precipitation and snowfall, we also express variability using the coefficient of variation (CV). Total precipitation is most variable during autumn (CV = 30 percent) and least variable during summer (CV = 24 percent). Approximately 60 percent of annual snowfall occurs during winter, when the CV is 28 percent. Since total runoff is quite variable from season to season, we compare seasonal values using both standard deviation and CV. The standard deviations of total runoff during autumn, winter, and spring are comparable, but the CV is higher during winter (39 percent) because mean runoff is low. On an annual basis, the CV in runoff is 24 percent. Base flow (R_g) has relatively low variability compared to total runoff, with an annual CV of 8 percent and higher variability during autumn and winter (CV = 13–14 percent). Evapotranspiration has the lowest CV of all fluxes, with an annual value of 5 percent. During autumn, spring, and summer, when most evapotranspiration occurs, CVs are 11 percent, 12 percent, and 7 percent, respectively.

Contribution of Snow to Water Supplies

Although snowfall accounts for 21 percent and 18 percent, respectively, of total precipitation in the Can-

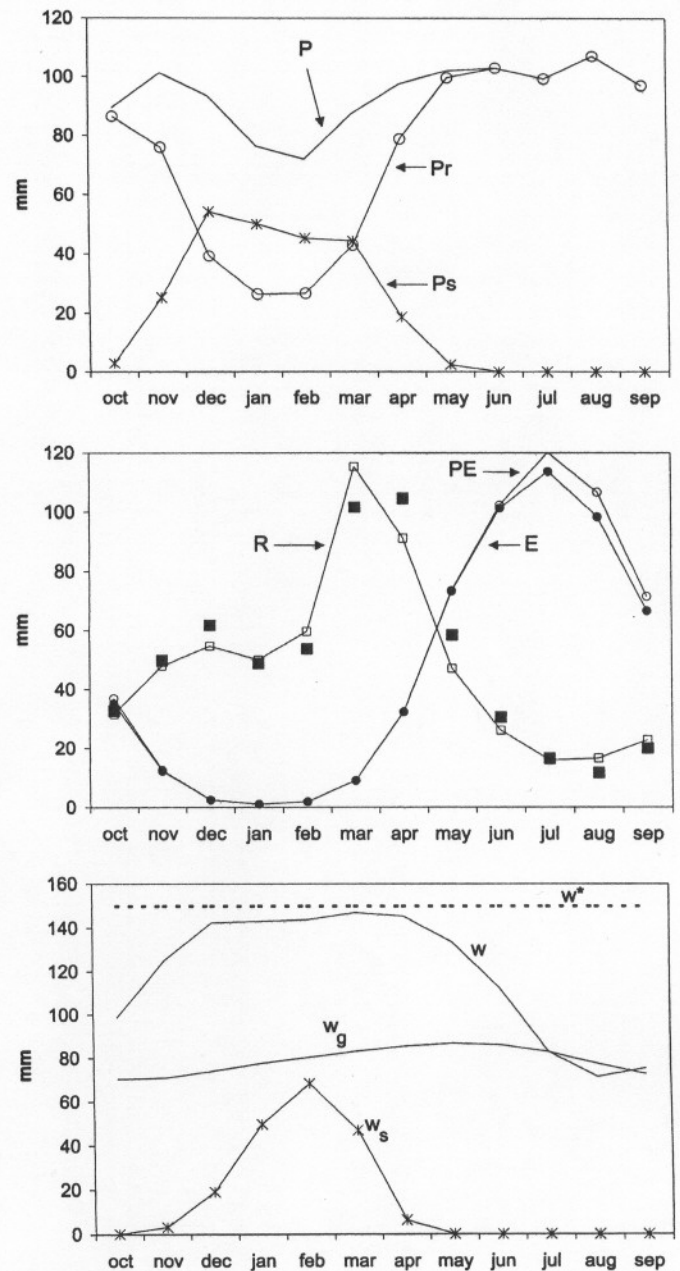


Figure 9. Modeled mean monthly water fluxes and water-reservoir levels in the Cannonsville watershed (1959–1988). The top panel shows total precipitation (P), rainfall (P_r), and snowfall (P_s). The middle panel includes total runoff (R), evapotranspiration (E), potential evapotranspiration (PE), and observed streamflow (closed boxes). The bottom panel includes the root-zone layer (w), root-zone-layer water capacity (w^*), groundwater layer (w_g), and snow pack (w_s). All values are in mm water equivalent.

nonsville and Ashokan basins (Table 3), the contribution of snow to runoff is substantially greater than the contribution of snowfall to total precipitation. Only water that enters the soil reservoir (w) is available for ET. When soils are saturated, precipitation and snow melt di-

Table 4. Cannonsville Basin Means (μ), Standard Deviations (σ), and Coefficients of Variation (CV) of Annual and Seasonal Temperature ($^{\circ}\text{C}$) and Water Fluxes (mm) (1957–1997)

	Annual			Sept.–Oct.–Nov.			Dec.–Jan.–Feb			Mar.–Apr.–May			Jun.–Jul.–Aug		
	μ	σ	CV (%)	μ	σ	CV (%)	μ	σ	CV (%)	μ	σ	CV (%)	μ	σ	CV (%)
T _{max}	13.2	0.6	—	14.6	1.1	—	-0.2	1.3	—	12.8	1.3	—	25.4	0.9	—
T _{min}	0.4	0.8	—	2.3	1.1	—	-11	1.9	—	-0.8	1.1	—	11	0.9	—
P	1137	174	15	294	87	30	243	65	27	291	60	21	310	73	24
P _r	897	158	18	266	82	31	95	45	47	227	58	26	310	73	24
P _s	240	61	25	27	23	85	148	41	28	64	30	47	0	0	0
ET	548	29	5	114	12	11	6	4	67	115	14	12	314	21	7
R	588	138	24	105	67	64	168	66	39	256	67	26	60	28	47
R _g	167	14	8	37	5	14	40	5	13	45	3	7	44	3	7

Note: CV is expressed as a percentage of the mean, $CV = \sigma * 100 / \mu$, where σ is the standard deviation and μ is the mean. — indicates not applicable.

rectly contribute to runoff and are not available for ET. Since a large portion of snow melt occurs in spring, when the soils are already saturated (Figure 9), much of it goes directly to runoff. To conservatively estimate the minimum magnitude of this effect, we assume that of the total annual snow melt (~240 mm), all snow melt that occurs between October and December (~60 mm) contributes to ET, while the snow melt that occurs after December (180 mm) contributes to runoff. This constitutes 31 percent of total runoff (588 mm). The same calculation over the Ashokan indicates that snow contributes about 24 percent to total runoff. Thus, the contribution of snow to runoff is at least 1.3 to 1.5 times the contribution of snow to total precipitation.

Interannual Variability

For the entire period of observation, mean annual runoff is 587 mm. The early 1960s were the driest period of the twentieth century over much of the northeastern U.S. During seven consecutive years, the streams shown in Figure 6 had streamflow <500 mm. The mid-1970s were the wettest period of the century in this region, with seven consecutive years of streamflow >700 mm.

The time series of annual water fluxes (Figure 10) reveals that precipitation over the Cannonsville basin (1957–1996) varies between 830 mm and 1600 mm annually. Most of this variability is due to rainfall (mean 900 mm, min 600 mm, max 1270 mm), with a lesser amount contributed by snowfall (mean \approx 240 mm, min 110 mm, max 400 mm). Higher precipitation (1400–2000 mm) over the Ashokan (not shown) reflects both the southeast to northwest precipitation gradient across the region and the high elevation of the Slide Mountain station. However, annual precipitation variations over the two basins are highly correlated ($r = 0.86$). Differences between the basins include a less persistent wet period of

the mid-1970s over the Ashokan. The model explains most of the interannual variability in streamflow ($r = 0.97$; see the fifth section of this article).

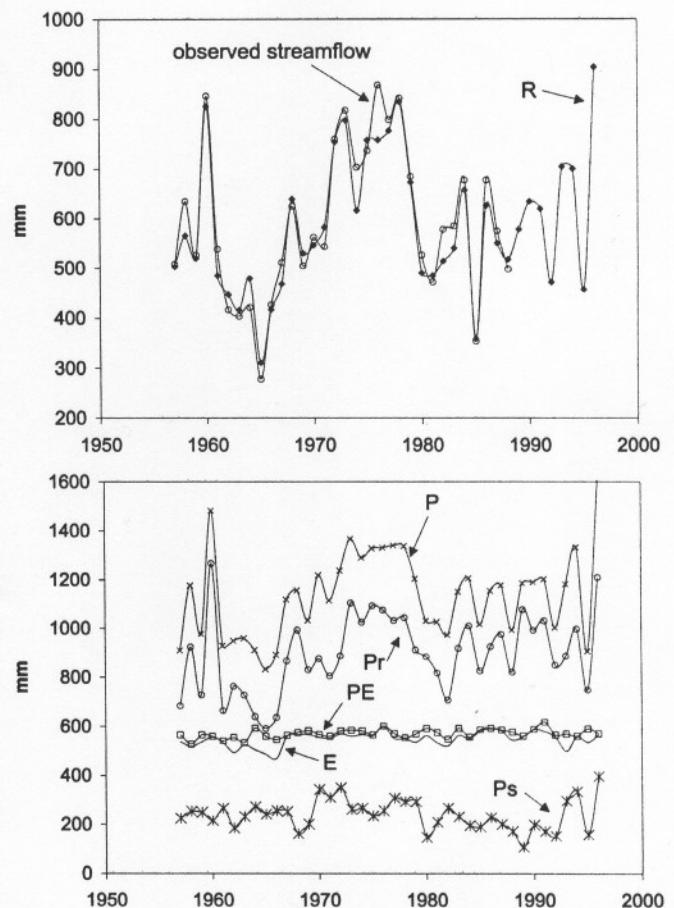


Figure 10. Time series of annual water fluxes. The top panel shows modeled total runoff (R, solid line) and observed streamflow (dashed line). The bottom panel shows total precipitation (P), rain (P_r), snowfall (P_s), evapotranspiration (E), and potential evapotranspiration (PE).

Figure 10 also indicates that the model estimates total annual streamflow remarkably well. However, we consider the level of accuracy indicated by this figure to be a bit deceptive, probably associated with a fortuitous compensation of errors in precipitation, evapotranspiration, and soil water-capacity. We would expect annual values to be within ± 10 percent, but a detailed assessment of these errors awaits model improvements and application to other basins.

Evapotranspiration as a Fraction of Precipitation

ET varies less than does snowfall, with an annual mean over the Cannonsville basin of ≈ 550 mm and extremes of 470 mm and 600 mm. ET varies between ≈ 35 percent and 60 percent of total precipitation over the Cannonsville (Figure 11), compared to 30–45 percent over the Ashokan. Lower values over the eastern basin occur because total precipitation is higher, while total ET and PE are comparable.

Dry (1961–1967) and Wet (1972–1978) Periods

In this section, we examine the mean water balance of the Cannonsville basin during the seven-year dry and wet periods. These will be used later to help us consider climate-change scenarios within the context of observed extremes. The cold drought of the 1960s was associated with anomalous northwesterly atmospheric flow over the northeastern U.S., while during the warm, moist 1970s southwesterly flow was more prevalent. These circulation patterns and associated temperature and precipitation departures are related to complex interactions be-

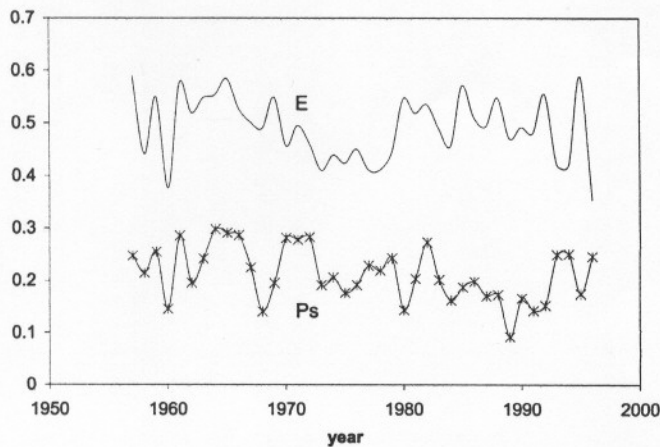


Figure 11. Evapotranspiration (E) and snowfall (Ps) expressed as a fraction of total precipitation.

tween long waves in the atmosphere and sea surface temperatures over the North Pacific and North Atlantic Oceans that modulate the location and strength of the eastern U.S. trough (Namias 1966, 1978; Douglas, Cayan, and Namias 1982; Diaz and Namias 1983). As a result, prevailing air masses and storm tracks near the eastern seaboard during these two periods were quite different.

As changes in ET were relatively small between these extreme periods (because temperature changes were relatively small), most observed runoff excesses or deficits were caused by precipitation fluctuations. During the drought, precipitation in the Cannonsville was approximately 945 mm yr^{-1} , a deficit of about 193 mm (17 percent below normal). Since ET was approximately normal during this period, these precipitation deficits translated into runoff deficits, resulting in streamflow measurements only 75 percent of normal over the Cannonsville.

Figure 12 shows monthly anomalies (the long-term mean subtracted from wet or dry period means) of water fluxes. During the dry period, precipitation was below normal in all months except January and August. The deficit was particularly pronounced during

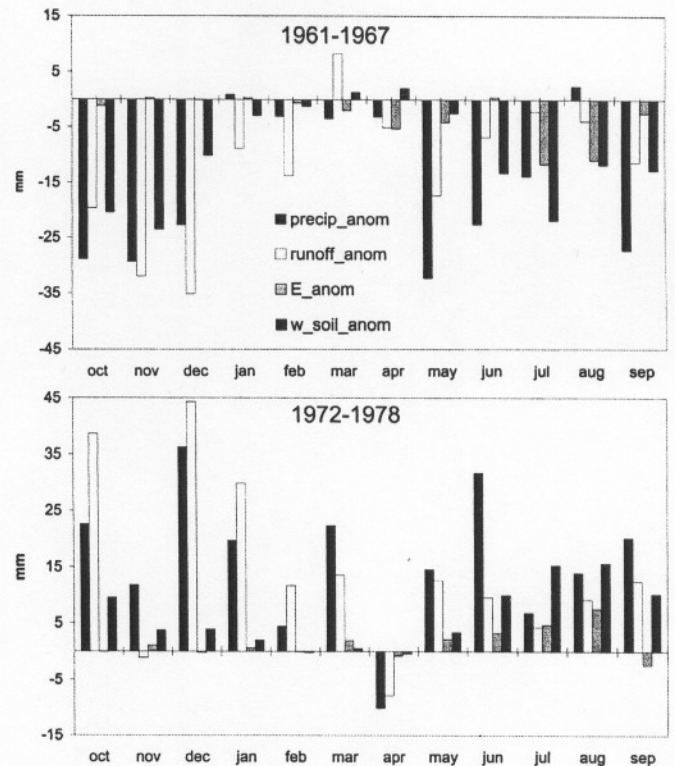


Figure 12. Water fluxes over the Cannonsville watershed for the driest (1961–1967) and wettest (1972–1978) periods of the last century expressed as anomalies with respect to the long-term (1959–1988) means. Shown are precipitation, total runoff, evapotranspiration, and soil moisture in the root-zone layer.

autumn and late spring/early summer. Soil moisture levels dropped significantly, especially during midsummer and autumn. Summer ET fell by ≈ 10 percent. As a result, total runoff was below the long-term mean for all months except March, especially between October and December.

During the wet period, precipitation was high for all months except April. Soil moisture and ET were particularly high during summer, when soil moisture is usually lowest. (During winter, soils are generally saturated and soil moisture anomalies are small). As a result, monthly runoff anomalies largely follow precipitation anomalies, except during summer, when increased ET removes some of the excess precipitation from the basin. During this period, mean annual precipitation was 1320 mm, 16 percent above normal, while annual mean runoff was approximately 30 percent above normal. During the wet period, temperatures were slightly above normal ($\approx +0.2^\circ\text{C}$), while during the dry 1960s they were slightly below normal ($\approx -0.4^\circ\text{C}$).

In the next section we show that, in contrast to observed twentieth-century fluctuations, projected changes during the twenty-first century are caused by temperature (hence evapotranspiration) as well as precipitation changes. These projected changes are outside the range of observed twentieth-century variations.

Climate Change

Prior to examining the potential impacts on water supply of specific climate-change scenarios derived from GCM results, we present a series of analyses to demonstrate the sensitivity of water supplies to temperature and precipitation changes.

Sensitivity

Due to the memory of the system contained in the snow and soil moisture reservoirs, changes in temperature and precipitation during one season can affect runoff during subsequent seasons. Figure 13 illustrates the effect of changing the daily temperature by $\pm 2^\circ\text{C}$ during each season, a change equivalent to between 1 and 2σ . An increase in winter (DJF) temperature causes pronounced increases in winter runoff and decreases in spring runoff due to the increased rain:snow ratio and increased snow melt during winter. A decrease in winter temperatures has the opposite effect: winter runoff decreases, but spring runoff increases. Increased spring temperatures cause an earlier spring melt, while decreased spring temperatures delay the melt period. The changes shown here are on the order of several weeks. Changes in

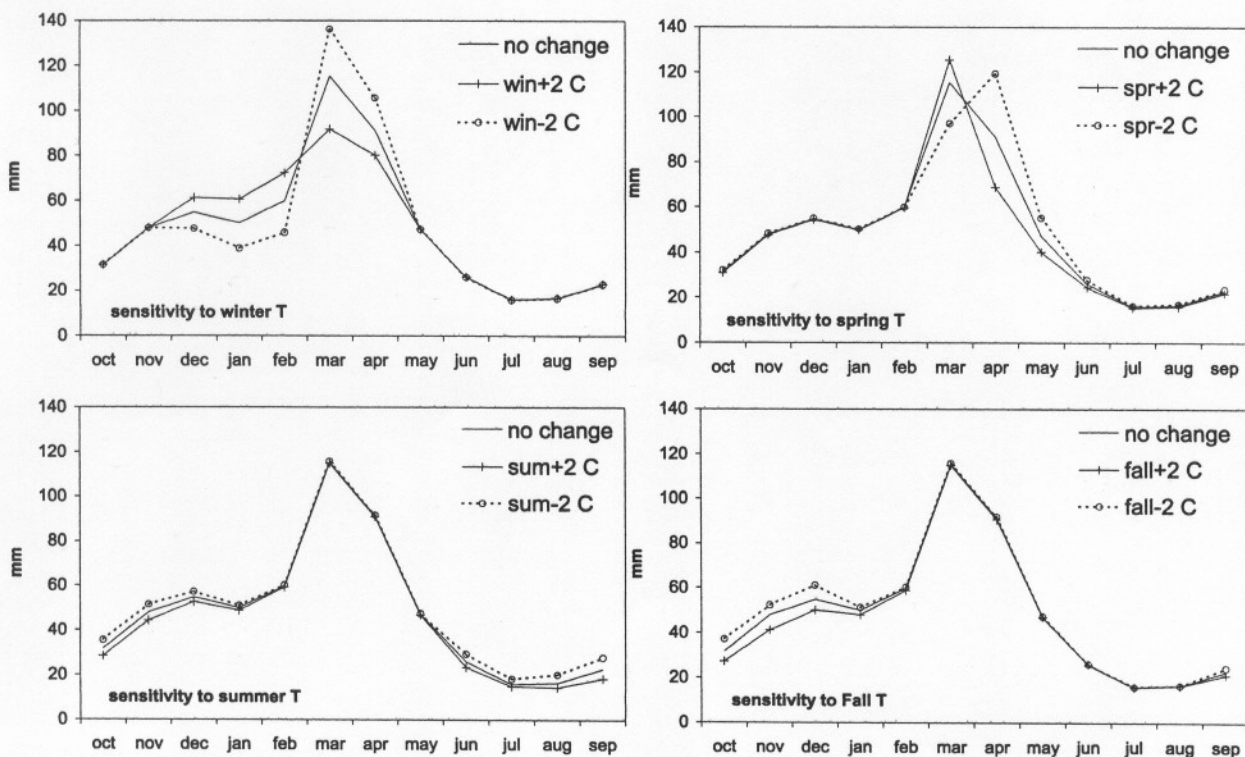


Figure 13. Sensitivity of the annual runoff cycle to seasonal temperature changes. Each panel shows modeled monthly mean runoff for the control case and for seasonal temperature changes of $\pm 2^\circ\text{C}$.

temperature during summer affect both summer and autumn runoff, due to the effects on soil moisture. Autumn temperature changes can influence runoff well into the winter season. Total annual runoff is least sensitive to winter temperatures when little ET occurs.

Alterations in seasonal precipitation (Figure 14) also have pronounced lagged effects. For example, a change in winter precipitation by ± 25 percent (equivalent to about 1σ) will affect monthly runoff by $\approx 10 \text{ mm mo}^{-1}$ into March and April. Changes in summer and autumn precipitation affect runoff into early winter. In addition, changes in autumn precipitation of ± 25 percent can affect runoff during that season by > 50 percent. Due to the saturated state of the surface soil layer in spring, any surplus or deficit in spring precipitation immediately affects runoff, precluding lagged effects during subsequent months.

To explore the combined effects of annual changes in temperature and precipitation, we ran the model with a series of simultaneous perturbations. For temperature we added the following values to each daily mean value: $\{-4^\circ\text{C}, -2^\circ\text{C}, 0^\circ\text{C}, +2^\circ\text{C}, +4^\circ\text{C}\}$. We multiplied daily precipitation and snowfall amounts by $\{0.5, 0.75, 1, 1.25, 1.5\}$. Thus, the model was run for a total of $5 \times 5 = 25$ cases. Figure 15 shows a surface plot of changes in total annual runoff associated with these combinations. For

example, the point where the $P \times 1.25$ and $T - 2$ lines cross shows a value between $+50$ percent and $+75$ percent. This indicates that under conditions of a 25 percent precipitation increase and 2°C temperature decrease, annual runoff increases between 50 percent and 75 percent. However, a similar precipitation increase combined with a 2°C temperature increase ($T + 2$) increases mean annual runoff from current conditions by only 25 percent to 50 percent, due to increased ET in the warmer scenario. The sensitivity to temperature changes is approximately ± 25 percent change in runoff for temperature changes of $\pm 4^\circ\text{C}$. Similarly, a change in precipitation of ± 50 percent affects runoff by ± 75 –90 percent.

Figure 15 also shows results based on conditions during the dry and wet periods detailed above. As discussed in the previous section of this article, mean precipitation for those periods deviated from normal by more than 15 percent, with corresponding temperature anomalies of $\approx -0.4^\circ\text{C}$ during dry years and $+0.2^\circ\text{C}$ during wet years. Observed (modeled) runoff changes for 1961–1967 are approximately -28 percent (-25 percent); those for 1972–1978 are $+34$ percent ($+31$ percent). Thus, the model simulates the mean annual runoffs—within ± 3 percent—that were observed during the most extreme precipitation periods in the observational record.

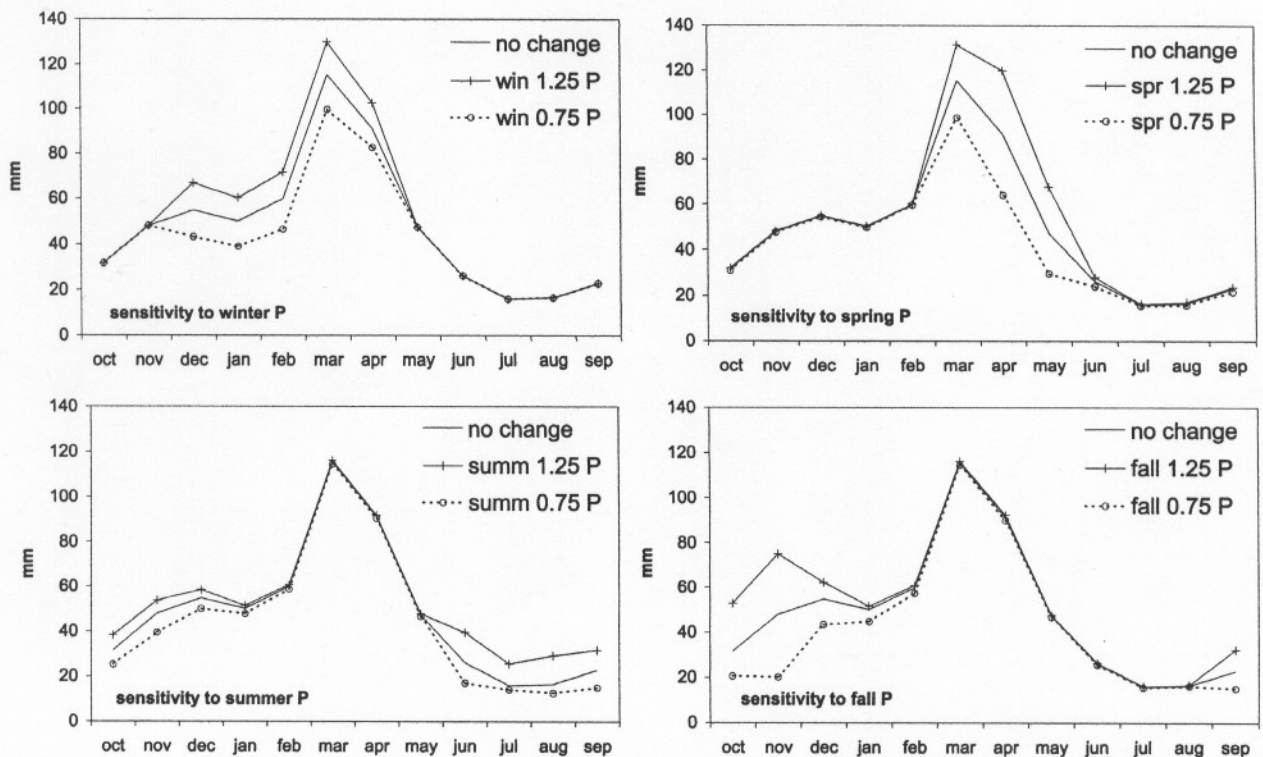


Figure 14. Sensitivity of the runoff cycle to seasonal precipitation changes. Each panel shows modeled monthly mean runoff for the control case, and for seasonal precipitation changes of ± 25 percent.

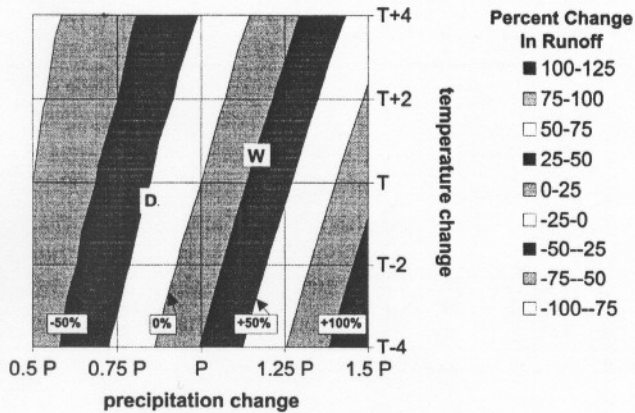


Figure 15. Sensitivity of total annual runoff to annual temperature and precipitation changes in the Cannonsville watershed. Runoff changes are in percent of the mean, precipitation changes are in the fraction of the mean, and temperature changes are in °C. To read the chart, pick a temperature change (e.g., for a 2°C increase, choose T+2) and a precipitation change (e.g., for a 25 percent increase, choose 1.25 P) and read the pattern-coded value of percent change in total annual runoff from chart. Also shown are the approximate locations of the dry period (1961–1967) (D) and wet period (1972–1978) (W).

Climate-Change Scenarios

Using GCM temperature and precipitation projections, one can obtain projected changes in annual mean water supply by the end of the twenty-first century that are comparable in magnitude to the extreme values observed during the 1960s and 1970s. Seasonal projections are even more dramatic. In an earlier study, Broccoli (1996) used GCM results to estimate that by 2030, winter temperatures over the New York City metropolitan

region may increase up to 3°C, with summer increases up to 2°C. Winter (summer) precipitation may increase 0–15 percent (5–10 percent). Over the Cannonsville, such changes are on the order of $>1\sigma$ for temperature, and $>1\sigma$ for precipitation (Table 4). By 2070, Broccoli estimated, even larger changes will occur.

Here we calculate the water balance for more recent climate-change scenarios developed for the IPCC and used by the national and MEC assessments: current trend, HHGG, HHGS, CCGG, and CCGS (see the third section, above, for detailed description). These scenarios include: a continuation of the linear trend fitted to the previous century's temperature and precipitation observations; results from two models (HH and CC); scenarios for greenhouse gases only (GG); and scenarios for greenhouse gases combined with sulphate aerosols (GS). The water balance model is run using temperature and precipitation changes estimated from the model grid point located closest to directly above the basin, which are input on a monthly basis.

Projections from the two models differ substantially (Table 5). While both models project rising temperatures during the coming century at a rate faster than that during the twentieth century, the CC model predicts a more rapid temperature increase. Total annual precipitation changes predicted by the HH model are large and positive (i.e., more precipitation than currently), while the CC model predicts little change in total annual precipitation. Differences between the two model results on monthly time scales are also striking (Figure 16). The CC model warming is extreme during winter, with projected changes between 6°C and 8°C by the 2080s. During other seasons, CC projects warming between 4–6°C,

Table 5. Changes in Runoff Calculated by the Water-Balance Model for the Cannonsville Basin Associated with Three MEC Assessment Climate-Change Scenarios

Scenario	2020s		2050s		2080s	
	T, P	Runoff	T, P	Runoff	T, P	Runoff
Current trend	T +0.44 P +1%	-1%	T +0.78 P +1.6%	-2%	T +1.11 P +2.3%	-3%
HCGG	T +1.6 P +4.5%	-1%	T +2.6 P +12.9%	+7%	T +3.7 P +18.6%	+10%
HCGS	T +0.92 P +4.8%	+3%	T +1.6 P +7.6%	+3%	T +2.6 P +15.8%	+12%
CCGG	T +1.7 P +0.2%	-10%	T +3.5 P -4.5%	-27%	T +5.3 P +2.4%	-28%
CCGS	T +1.7 P -0.4%	-11%	T +3 P +0.1%	-19%	T +4.8 P +0.9%	-28%

Note: The current-trend scenario assumes the continuation of linear temperature and precipitation trends observed in the twentieth century, 0.11°C/decade (0.2°F/decade) and 0.25 cm/decade (0.1 inch/decade). HCGS and CCGS are results from two GCMs that include the effects of increased greenhouse gases as well as aerosols. See text for further discussion of scenarios. Runoff changes are expressed as percentage change in total annual runoff compared to the base period, 1959–1988. Water-balance results assume that the temperature and precipitation changes are distributed evenly throughout the year, and that no change in variability occurs.

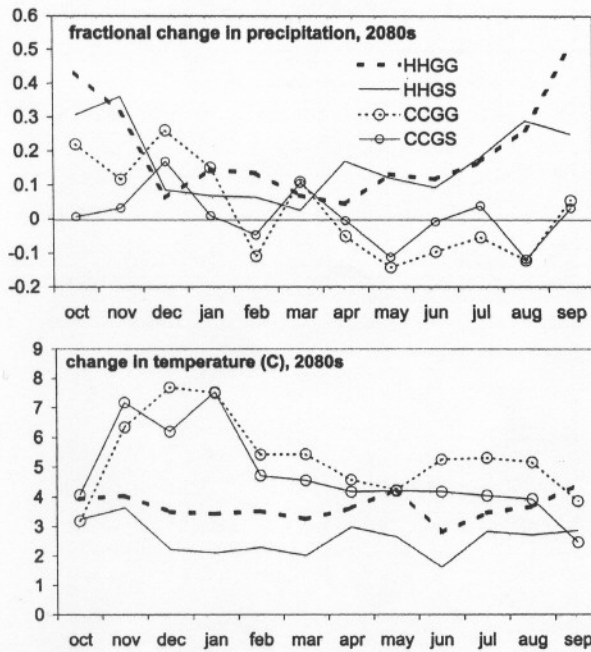


Figure 16. Projected temperature and precipitation changes for the 2080s for different climate-change scenarios taken from GCM experiments (HHGG, HHGS, CCGG, CCGS) described in the third section of this article. These values were used as input into the water-balance model.

still higher than HH projections of 2–4°C monthly mean warming by the 2080s. The HH model projects large precipitation increases over this region, particularly during late summer/early autumn, when, depending on the scenario, precipitation will increase between 25 percent and 50 percent by the 2080s. In contrast, the CC model shows potentially moderate increases (0 to 25 percent) during the first half of the water year, and possibly

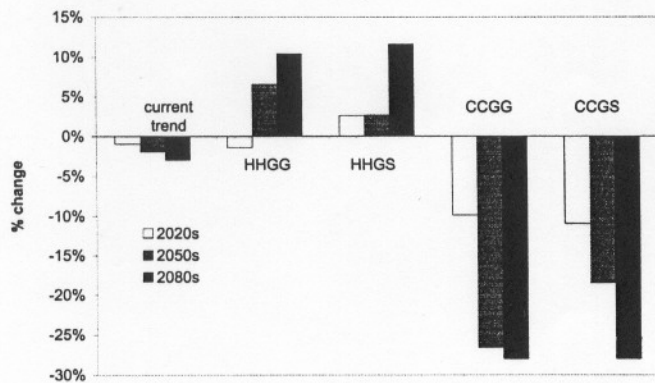


Figure 17. Projected annual mean runoff changes in the Cannonsville Basin for five different climate-change scenarios taken from GCM experiments (HHGG, HHGS, CCGG, CCGS) described in the third section of this article. Results are shown for the 2020s (no shading), 2050s (light shading), and 2080s (dark shading).

moderate decreases (–15 to +5 percent) in precipitation during the latter half.

Uncertainty due to disagreement in precipitation between models is not unique to this region. Indeed, it has been identified across the U.S. for the HH and CC models used in the national assessment (Kerr 2000), as well as in earlier hydrological studies across the U.S. (McCabe and Ayers 1989; Wolock and Hornberger 1991; Lettenmaier et al. 1999). Similar uncertainties were also found in higher-latitude basins in Canada, where models are often assumed to be in better agreement on precipitation increases associated with global warming (Cohen, Welsh, and Louie 1989).

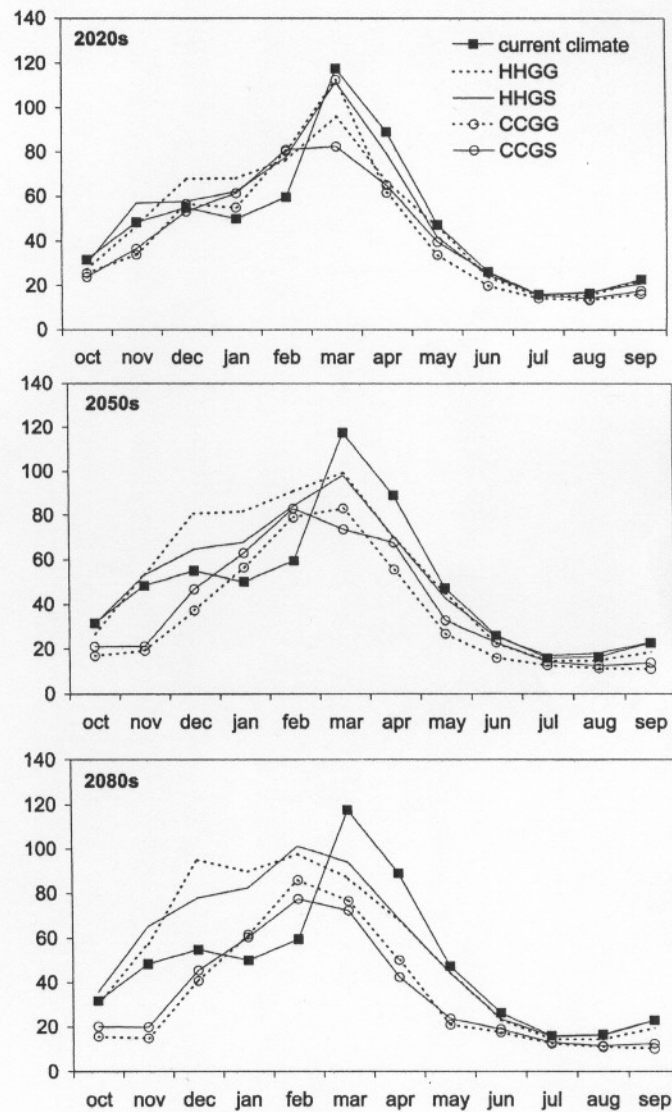


Figure 18. Projected monthly mean runoff values estimated by the water-balance model. Climate-change scenarios for the 2020s, 2050s, and 2080s were taken from GCM experiments (HHGG, HHGS, CCGG, CCGS) described in the third section of this article. Units are mm of water equivalent.

As a result of these differences, annual mean runoff changes estimated by the water balance model using the aforementioned scenarios vary widely (Figure 17). In the current-trend scenario, relatively moderate temperature increases, which lead to increased evapotranspiration and decreased runoff, are mostly offset by moderate precipitation increases, so that the net effect on annual runoff is minimal (decreases of less than 5 percent). HH model projections produce moderate increases in runoff (up to around 12 percent) by the 2080s. CC model projections, on the other hand, result in moderately decreased runoff by the 2020s (-10 percent), with much larger reductions (close to -30 percent) by the 2080s.

During the most extreme wet and dry periods of the twentieth century (see the sixth section of this article), mean annual temperature departures were under ± 0.5 C, and changes in runoff were affected mainly by precipitation departures. However, twenty-first-century projections from both the HH and CC models indicate substantial warming. While precipitation increases projected by the HH model are comparable to those observed during the wet 1970s, under the warmer climate increased evapotranspiration will partially offset rising precipitation rates,

resulting in runoff increases of only +12 percent, compared to +30 percent observed during the 1970s. In contrast, the CC model projects only minor changes in annual precipitation amounts, which in tandem with increased temperatures results in increasingly drier conditions throughout the twenty-first century. By the end of the century, if these projections pan out, runoff under mean climatic conditions will be comparable to that of the drought years of the 1960s.

Equally important to annual mean changes are potential alterations to the seasonal cycle (Figure 18). Only moderate changes to the bimodal annual runoff cycle (i.e., spring peak/winter secondary peak) are expected during the next two to three decades. However, by the 2050s we find runoff spread more evenly across the winter and spring months, with a weaker spring peak. By the 2080s, the HH scenarios indicate increased winter runoff (>+50 percent) and decreased spring runoff (-25 percent). Projections from the drier CC model also indicate a late winter or early spring peak. The primary reason for this is the altered snow-pack associated with warmer climates (Figure 19). According to these projections, peak snow-pack will be diminished by more than half in all

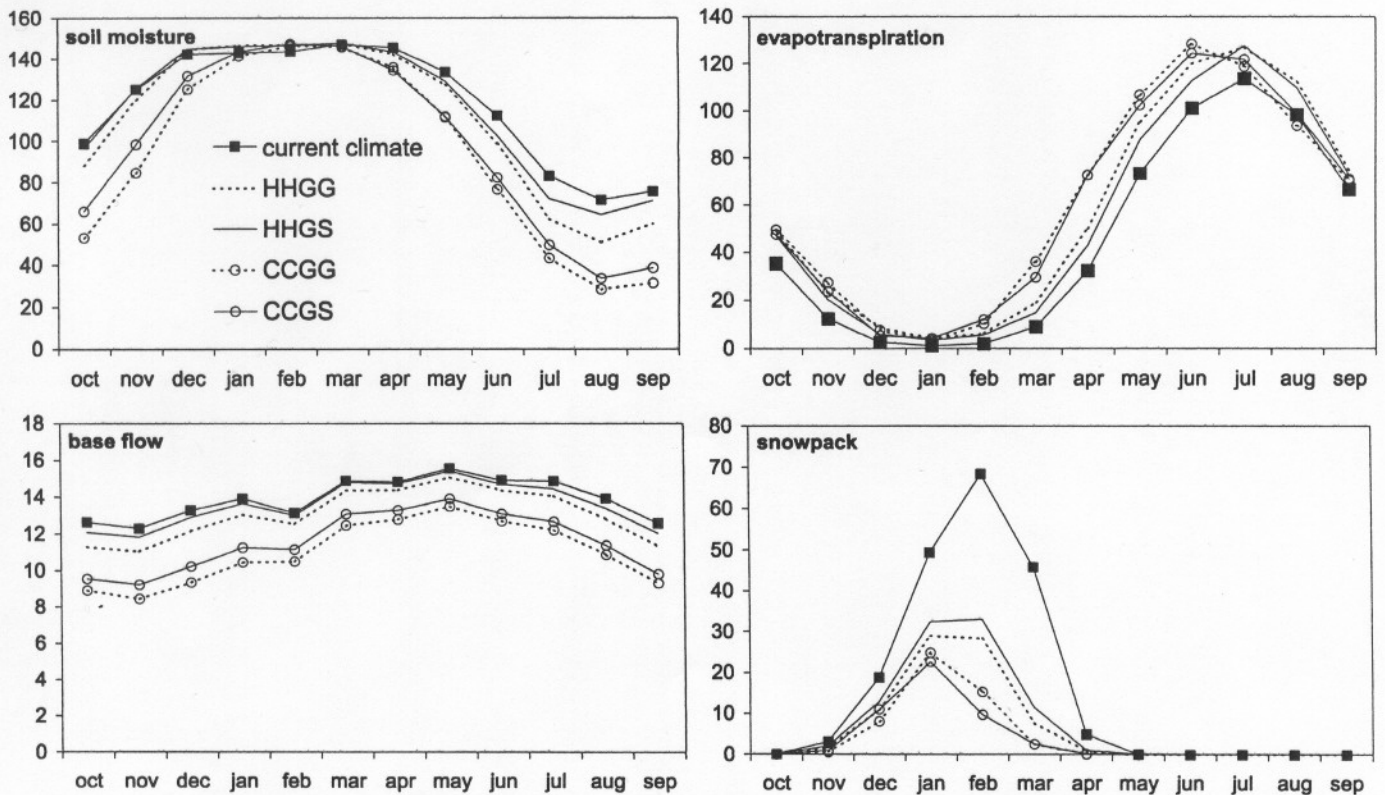


Figure 19. Projected monthly mean values of soil moisture, evapotranspiration, base flow, and snow pack estimated by the water-balance model for the 2080s. Climate-change scenarios were taken from GCM experiments (HHGG, HHGS, CCGG, CCGS) described in the third section of this article. Units are mm of water equivalent.

scenarios. In addition, all scenarios produce increased evapotranspiration, especially during spring and early summer, as well as decreased soil moisture, ground water, and base flow (Figure 19). In all scenarios, by the 2080s the annual runoff cycle will be significantly modified, with a markedly diminished snow pack and with peak flow shifted earlier in the season.

Summary and Conclusions

We used a version of the Thornthwaite (1948) water-balance model to estimate the seasonal cycle, interannual variations, and sensitivity to climate change of water fluxes for a watershed in the Catskill Mountains. This region supplies water to approximately 10 million people in and around New York City, as well as to users of Delaware River water in New Jersey and Pennsylvania. The Cannonsville basin was chosen because it represents the western, or Delaware, basin, which supplies 50 percent of New York City's water; and because of the availability of a long unbroken series of meteorological observations (1957–1996). This dataset allowed us to examine the water balance for a variety of conditions, including the driest (early to mid-1960s) and wettest (mid-1970s) periods of the twentieth century, as well as climate-change scenarios employed by national and regional climate-change assessments.

Historically, approximately half of total precipitation over the western Catskills is lost to evapotranspiration, which is usually at or close to its potential during all months. The contribution of snow to runoff is approximately 1.5 times the proportion of total annual precipitation that falls as snow. In addition to the spring runoff peak associated with snow melt, a secondary winter peak is found in both observations and model results as a consequence of the interplay between the seasonal cycles of solid and liquid precipitation and temperature. These features of the annual runoff cycle can potentially be altered dramatically under future climate-change scenarios.

Using the water-balance model to perform sensitivity experiments, we found that the sensitivity of water supply to temperature changes is approximately 6 percent per °C for mean annual values. The sensitivity of water supply to precipitation changes is less linear, but varies between 1.5 percent and 2 percent per percent change in precipitation. Thus, the change in mean annual precipitation in the Cannonsville Basin required to offset a temperature change (i.e., to maintain the mean historical runoff volume into the reservoir) is approximately 3–4 percent per °C. The seasonal water-cycle is particularly sensitive to winter and spring temperature changes, which affect the storage and subsequent release of water

from the snow pack, and to winter and summer precipitation changes, which have significant lagged effects well into subsequent seasons.

When using the water-balance model in conjunction with GCM-based climate-change scenarios, we found substantial alterations of the hydrologic cycle. Future climate projections from the two models differ significantly with regards to total annual precipitation rate as well as to the annual temperature cycle. All scenarios indicate a warming, and although the magnitudes and seasonal distributions vary, the warming is consistently sufficient to increase evapotranspiration substantially, to decrease runoff, and to offset a large portion of any increase in precipitation that may occur. As a result, twenty-first-century water supplies are likely to decrease, and any increases are likely to be moderate at best. In the worst scenario examined here, by the latter half of the twenty-first century runoff under mean climatic conditions will be comparable to that of the dry period during the 1960s.

Although only moderate changes to the seasonal runoff cycle are expected during the early years of this century, under all scenarios a drastically altered seasonal cycle will later become apparent. Largely the result of a diminishment of the winter snow pack by at least 50 percent, by the latter half of the century more runoff will occur during winter, and peak runoff will occur one to two months earlier than under current climatic conditions.

These projections portend substantial changes in the amount and timing of Catskill water supplies. How serious a problem may this be? While a conservative estimate of population growth in New York City indicates at least a 30 percent increase by 2080 over the year 2000 population of eight million,² which is likely to be accompanied by increased demand, the severity of the problem will depend on a number of additional issues. These include: the sign and magnitude of precipitation changes; changes in the distribution of extreme events; adaptive capabilities of reservoir operations; changes in per-capita consumption; and potential interbasin transfers. In any case, if temperatures rise without a simultaneous and sufficient increase in precipitation, the region will experience diminished supplies. Even under the best scenario employed by the national and regional assessments, in which a water-supply increase on the order of 10 percent is projected, it may be difficult to maintain demand at a sustainable level.

Acknowledgments

This work was supported by NASA grants NAG5-7543, NAG5-7496, and NAG13-99005; and NSF grant

EAR9634329. Special thanks to Andrew Barrett for numerous helpful discussions. The authors also thank D. Robinson and J. Woo at Rutgers University for providing data, T. Spies at the New York City Department of Environmental Protection (DEP) for providing boundary files, R. Hurwitz at the DEP for discussions, and three anonymous reviewers.

Notes

1. However, these issues are critical for policy development, and resources on them exist. A recent National Research Council (NRC) report provides a thorough overview of historical, environmental, and management issues associated with the New York City water supply (NRC 2000). Platt, Marten, and Pfeffer (2000) provide a more condensed overview that includes a summary of the major NRC findings. Further information is available on history (Galusha 1999), environmental issues (Goldstein and Izeman 1990), and management issues (Marx and Goldstein 1993). With regard to climate change in the metropolitan region, in addition to the MEC assessment (Rosenzweig and Solecki 2001a, 2001b), see Hill (1996) and Major (1993).
2. This assumes exponential growth rate determined by 1980–1990 rate of change. 1990–2000 rate of change was not used, because large immigration during that decade makes the large growth rate unsustainable (I. Miyares, personal communication via conversation, 2001).

References

- Alley, W. M. 1984. On the treatment of evapotranspiration, soil moisture accounting, and aquifer recharge in monthly water balance models. *Water Resources Research* 20 (8): 1137–49.
- Andersson, L. 1992. Improvements in runoff models: What way to go? *Nordic Hydrology* 23:315–32.
- Arnell, N. 1996. *Global warming, river flows, and water resources*. Chichester: John Wiley & Sons.
- Broccoli, A. J. 1996. The greenhouse effect: The science base. In *Annals of the New York Academy of Sciences: The baked apple: Metropolitan New York in the greenhouse*, ed. D. Hill, 790:19–28. New York, The New York Academy of Sciences.
- Burns, D. A., G. B. Lawrence, and P. S. Murdoch. 1998. Streams in Catskill Mountains still susceptible to acid rain. *EOS* 79 (16):197.
- Cohen, S. J., L. E. Welsh, and P. Y. T. Louie. 1989. *Possible impacts of climatic warming scenarios on water resources in the Saskatchewan River subbasin*. Report no. 89–9. Saskatoon, Saskatchewan: Canadian Climate Centre, Atmospheric Environment Service, National Hydrology Research Centre.
- Diaz, H. F., and J. Namias. 1983. Associations between anomalies of temperature and precipitation in the United States and western northern hemisphere 700-mb height profiles. *Journal of Climate and Applied Meteorology* 22:352–62.
- Doesken, N. J., and A. Judson. 1997. *The snow booklet: A guide to the science, climatology, and measurement of snow in the United States*. Fort Collins, CO: Colorado Climate Center, Department of Atmospheric Science, Colorado State University.
- Douglas, A. V., D. R. Cayan, and J. Namias. 1982. Large-scale changes in North Pacific and North American weather patterns in recent decades. *Monthly Weather Review* 110:1851–62.
- Federer, C. A., C. Vorosmarty, and B. Fekete. 1996. Intercomparison of methods for calculating potential evaporation in regional and global water balance models. *Water Resources Research* 32 (7): 2315–21.
- Galusha, D. 1999. *Liquid assets: A history of New York City's water system*. Fleischmanns, NY: Purple Mountain Press.
- Gleick, P. H. 2001. Global water: Threats and challenges facing the United States. *Environment* 43 (2): 18–26.
- Goldstein, E. A., and M. A. Izeman. 1990. *The New York environment book*. New York: NRDC: Washington, DC: Island Press.
- Groisman, P. Y., and D. R. Legates. 1994. The accuracy of United States precipitation data. *Bulletin of the American Meteorological Society* 75 (3): 215–26.
- Groopman, A. 1967. Effects of the northeast water crisis on the New York City water supply system. *Journal of the American WaterWorks Association* 60:37–48.
- Hendrick, R. L., and R. J. DeAngelis. 1976. Seasonal snow accumulation, melt and water input—A New England model. *Journal of Applied Meteorology* 15:717–27.
- Hill, D., ed. 1996. *The baked apple: Metropolitan New York in the greenhouse*. Annals of the New York Academy of Sciences. New York: New York Academy of Sciences.
- Intergovernmental Panel for Climate Change (IPCC). The IPCC data distribution centre. <http://ipcc-ddc.cru.uea.ac.uk/> (last accessed 31 January 2002).
- Jakeman, A. J., and G. M. Hornberger. 1993. How much complexity is warranted in a rainfall-runoff model? *Water Resources Research* 29 (8): 2637–49.
- Judson, A., and N. Doesken. 2000. Density of freshly fallen snow in the central Rocky Mountains. *Bulletin of the American Meteorological Society* 81 (7): 1577–87.
- Karl, T. R. 1983. Some spatial characteristics of drought duration in the United States. *Journal of Climate and Applied Meteorology* 22:1356–66.
- Kerr, R. A. 2000. Dueling models: Future U.S. climate uncertain. *Science* 288 (5474): 2113.
- Kustas, W. P., A. Rango, and R. Uijlenhoet. 1994. A simple energy budget algorithm for the snowmelt runoff model. *Water Resources Research* 30 (5): 1515–27.
- Leffler, R. J. 1981. Estimating average temperatures on Appalachian Summits. *Journal of Applied Meteorology* 20:637–42.
- Legates, D. R., and T. L. DeLiberty. 1993. Precipitation measurement biases in the United States. *Water Resources Bulletin* 29 (5): 855–61.
- Legates, D. R., and J. R. Mather. 1992. An evaluation of the average annual global water balance. *The Geographical Review* 82 (3): 253–67.
- Lettenmaier, D. P., A. W. Wood, R. N. Palmer, E. F. Wood, and E. Z. Stakhiv. 1999. Water resources implications of global warming: A U.S. regional perspective. *Climatic Change* 43:537–79.
- Lindstrom, G., B. Johansson, M. Persson, M. Gardelin, and S. Bergstrom. 1997. Development and test of the distributed HBV-96 hydrological model. *Journal of Hydrology* 201:272–88.
- Lockwood, J. G. 1999. Is potential evapotranspiration and its relationship with actual evapotranspiration sensitive to elevated atmospheric CO₂ levels? *Climatic Change* 41 (2): 193–212.
- Major, D. C. 1993. The water supply system of New York City and global climate change. In *Proceedings of the First Na-*

- tional Conference on Climate Change and Water Resources Management, U.S. Army Corps of Engineers, ed. Thomas M. Ballentine and Eugene Z. Stakhiv, 11-130-139. IWR Report 93-R-17.
- Martin, M., R. E. Dickinson, and Z-L. Yan. 1999. Use of a coupled land surface General Circulation Model to examine the impacts of doubled stomatal resistance on the water resources of the American Southwest. *Journal of Climate* 12 (12): 3359-75.
- Marx, R., and E. A. Goldstein. 1993. *A guide to New York City's reservoirs*. New York: Natural Resources Defense Council.
- Mather, J. R. 1981. Using computed stream flow in watershed analysis. *Water Resources Bulletin* 7 (3): 474-82.
- . 1985. The water budget and the distribution of climates, vegetation, and soils. *Publications in Climatology* XXXVIII (2): entire issue.
- McCabe, G. J., and M. A. Ayers. 1989. Hydrologic effects of climate change in the Delaware River Basin. *Water Resources Bulletin* 25 (6): 1231-42.
- Milly, P. C. D. 1994. Climate, soil water storage, and the average annual water balance. *Water Resources Research* 30 (7): 2143-56.
- Mintz, Y., and Y. V. Serafini. 1992. A global monthly climatology of soil moisture and water balance. *Climate Dynamics* 8:13-27.
- Mintz, Y., and G. K. Walker. 1993. Global fields of soil moisture and land surface evapotranspiration derived from observed precipitation and surface air temperature. *Journal of Applied Meteorology* 32:1305-34.
- Muller, R. A. 1969. Water balance evaluation of effects of subdivisions on water yield in Middlesex County, New Jersey. *Proceedings, Association of American Geographers* 1:121-25.
- . 1981. The water budget as a tool for inventory and analysis of factors affecting variability and change of river regime. In *The environment: Chinese and American views*, ed. L. J. C. Ma and A. G. Noble, 171-86. New York: Methuen and Co Ltd.
- Muller, R. A., and G. J. McCabe. 2000. A climatic water-budget interpretation of the 1999 Northeastern drought. Paper presented at the Annual Meeting of the Association of American Geographers, April, Pittsburgh, PA.
- Namias, J. 1966. Nature and possible causes of the northeastern United States drought during 1962-65. *Monthly Weather Review* 94 (9): 543-54.
- . 1978. Multiple causes of the North American abnormal winter 1976-77. *Monthly Weather Review* 106 (3): 279-95.
- National Research Council (NRC). 2000. *Watershed management for potable water supply: Assessing the New York City strategy*. Washington, DC: National Academy Press.
- New York City Department of Environmental Protection (DEP). 2001. Drought watch declared for New York City water supply. Press release, 27 December. <http://www.nyc.gov/html/dep/html/press/01-64pr.html> (last accessed 13 February 2002).
- Platt, R. H., P. K. Barten, and M. J. Pfeffer. 2000. A full, clean glass? Managing New York City's watersheds. *Environment* 42 (5): 8-21.
- Rosenzweig, C., and W. D. Solecki. 2001a. Climate change and a global city: Learning from New York. *Environment* 43 (3): 8-18.
- Rosenzweig, C., and W. D. Solecki, eds. 2001b. *Climate change and a global city: The Metropolitan East Coast Regional Assessment*. New York City: Columbia Earth Institute. <http://metroeast-climate.ciesin.columbia.edu/index.html> (last accessed 13 February 2002).
- Slack, J. R. S., A. M. Lumb, and J. M. Landwehr. 1993. Hydroclimatic data network (HCDN) streamflow data set, 1874-1988. USGS Water-Resources Investigations Report. Reston, VA: USGS.
- Thaler, J. S. 1989. Hudson Basin precipitation regimes: Croton, Esopus, and Schoharie watersheds. *Northeastern Environmental Science* 8:106-18.
- . 1994. Climate of Albany County. *Northeastern Geology* 16 (3&4): 162-93.
- . 1996. *Catskill weather*. Fleischmanns, NY: Purple Mountain Press.
- Thornthwaite, C. W. 1948. An approach toward a rational classification of climate. *Geographical Review* 38:55-94.
- Thornthwaite, C. W., and J. R. Mather. 1955. The water balance. *Publications in Climatology* 8 (1): 9-33.
- Thornthwaite, C. W., and J. R. Mather. 1957. Instructions and tables for computing potential evapotranspiration and the water balance. *Publications in Climatology* X (3): entire issue.
- USGS Earth Resources Observation Systems Data Center Distributed Active Archive Center (EDS DAAC). 2001. <http://edcdaac.usgs.gov/gtopo30/gtopo30.html> (last accessed 31 January 2002).
- U.S. National Assessment. 2002. *The potential consequences of climate variability and change*. <http://www.usgcrp.gov/usgcrp/nacc/default.htm> (last accessed 13 February 2002).
- Vorosmarty, C. J., C. A. Federer, and A. L. Schloss. 1998. Potential evaporation functions compared on U.S. watersheds: Possible implications for global-scale water balance and terrestrial ecosystem modeling. *Journal of Hydrology* 207: 147-69.
- Weisman, R. A. 1985. The 1980-81 drought in southeastern New York. *American Meteorological Society* 66 (7): 788-94.
- Willmott, C. J., C. M. Rowe, and Y. Mintz. 1985. Climatology of the terrestrial seasonal water cycle. *Journal of Climatology* 5:589-606.
- Wolock, D. M., and G. M. Hornberger. 1991. Hydrological effects of changes in levels of atmospheric carbon dioxide. *Journal of Forecasting* 10:105-16.
- Wolock, D. M., and G. J. McCabe. 1999a. Estimates of runoff using water-balance and atmospheric general circulation models. *Journal of the American Water Resources Association* 35 (6): 1341-50.
- Wolock, D. M., and G. J. McCabe. 1999b. Explaining spatial variability in mean annual runoff in the conterminous United States. *Climate Research* 11:149-59.
- Wolock, D. M., G. J. McCabe, G. D. Tasker, and M. E. Moss. 1993. Effects of climate change on water resources in the Delaware River Basin. *Water Resources Bulletin* 29 (3): 475-86.